Published in final edited form as:

Neuroimaging Clin N Am. 2023 February ; 33(1): 11–41. doi:10.1016/j.nic.2022.07.001.

Neuroimaging Patterns of Intracranial Infections:

Meningitis, Cerebritis, and Their Complications

Michael Tran Duong, PhD[a], **Jeffrey D. Rudie, MD, PhD**[b], **Suyash Mohan, MD, PDCC**[a,*]

[a]Division of Neuroradiology, Department of Radiology, Perelman School of Medicine at the University of Pennsylvania, 3400 Spruce Street, Philadelphia, PA 19104, USA

[b]Department of Radiology, Scripps Clinic and University of California San Diego, 10666 Torrey Pines Road, La Jolla, CA 92037, USA

Keywords

Central nervous system; Infection; Meningitis; Cerebritis; Abscess; Ventriculitis; Neuroimaging; Glymphatics

INTRODUCTION

Neuroimaging is essential for the diagnosis, management, and monitoring of central nervous system (CNS) infections.[1,2] Although some radiographic features are shared across infectious and noninfectious causes, CNS infections often exhibit specific or classic imaging patterns. During the last 3 decades, mortality from meningitis has decreased by 21% despite incidence rising by 13%, demonstrating the positive impact of accessibility to clinical care and decision-making guided by noninvasive and perioperative neuroimaging.[3]

Here, we provide an overview of classic imaging patterns of meningitis, cerebritis, intracranial abscess, and ventriculitis. We survey techniques such as computed tomography (CT), MR imaging, MR spectroscopy (MRS), diffusion-weighted imaging (DWI) with apparent diffusion coefficient (ADC) maps, PET, and recent advances in neuroimaging, including the potential role of artificial intelligence (AI) in diagnosing CNS infections. Then we survey specific infectious causes organized by location: extra-axial, intra-axial, and mixed. Finally, we present complications and mimics of CNS infections, including noninfectious meningitis, neoplastic, autoimmune, and inflammatory processes. We encourage the reader to reference other articles in this issue of *Neuroimaging Clinics* for further information about certain specific organisms, locations, or situations.

ANATOMY

The brain is covered by 3 connective tissue membranes, or “meninges.” The outermost layer is the dura mater (or *pachymeninges*, meaning “tough membrane”), which includes the venous sinuses and the falx and tentorium. Underneath is the arachnoid and pia mater (which together comprise the *leptomeninges*, meaning “thin membrane”). The potential

*Corresponding author.: suyash.mohan@pennmedicine.upenn.edu.

space between the inner table of the skull and dura is the epidural space. The potential space between the dura and arachnoid is the *subdural space*, which contains the delicate cortical bridging veins and arachnoid granulations. The space between the arachnoid mater and the pial vessels attached to the cortex is the *subarachnoid space*, which is bathed in cerebrospinal fluid (CSF; Fig. 1); all are prone to infected pus collections.

PATHOPHYSIOLOGY OF CENTRAL NERVOUS SYSTEM INFECTION

There are 4 main routes of infectious spread to the brain and meninges.

1. Hematogenous dissemination from a distal infectious source is the most common path.
2. Direct inoculation (Fig. 2) occurs from trauma, iatrogenic lumbar puncture (LP), or neurosurgical interventions.
3. Local extension of infection is seen with sinusitis, orbital cellulitis, mastoiditis (Fig. 3), otitis media, or dental infection.
4. Spread along cranial nerves can occur by rabies, herpes simplex virus (HSV), and *Naegleria fowleri*.

Local extension is less common than hematogenous dissemination, although relatively straightforward to identify on imaging. Otomastoiditis is associated with adjacent abscesses of the temporal lobe and cerebellum (see Fig. 3), whereas frontal and ethmoid sinusitis and odontogenic infections are linked to frontal lobe abscess.[2]

There are additional, uncommon routes for infection as up to 40% of brain abscesses are cryptogenic.[4] The calvarial emissary veins are valveless and promote bacterial localization from superficial face and scalp infections to the CNS via retrograde thrombophlebitis causing subdural empyema and cavernous sinus thrombosis.[5] Iatrogenic spread includes neurosurgical incision, dural graft transplant, and LP with spread through meningeal spaces (see Fig. 2). The recently discovered brain meningeal lymphatic system in humans,[6] running alongside the dural venous sinuses, might provide a previously unrecognized route of infectious transmission. Such “glymphatics” are demonstrated by their enhancement with gadobutrol, a contrast agent with proclivity to extravasate into tissue but not with an intravascular contrast dye such as gadofosveset.[6] These venous and lymphatic routes may converge at the choroid plexus, wherein microbes can spread through subarachnoid and perivascular spaces via purulent or inflammatory exudates. Tissue invasion may trigger cytokine release by microglia and immune cells, which alters the integrity of the blood–brain barrier (BBB) and promotes extravasation of contrast from intravascular to subarachnoid spaces, leading to characteristic meningeal enhancement present in many CNS infections.[1,7,8]

MENINGEAL ENHANCEMENT AND MENINGITIS

There are several types of meningeal enhancement: from normal dural enhancement (Fig. 4) to abnormal enhancement (Fig 5). *Pachymeningeal enhancement* involves the dura (see Fig. 3; Figs. 6 and 7) and is more often associated with noninfectious processes such

as intracranial hypotension, meningiomas, metastasis, and granulomatous disease (Box 1). Intracranial hypotension can result in pachymeningeal enhancement post-LP in about 1% of patients,[9] whereby a reduction in CSF pressure causes a compensatory hydrostatic shift of fluid volume into subarachnoid space veins. This phenomenon arises from the *Monro-Kellie doctrine*.[10] With contrast administration, this expanded subarachnoid volume seems as either local or diffuse pachymeningeal enhancement as well as distended dural venous sinuses. Certain CNS infections (neurosyphilis, tuberculous meningitis) may seem as more focal areas of pachymeningeal enhancement.[1,11]

Leptomeningeal enhancement (Fig. 8), when pathologic, is thicker, longer, asymmetric and extends into the depth of the sulci and fills the subarachnoid spaces in sulci and cisterns (Box 2). Leptomeningeal enhancement is seen in 50% of meningitis cases and has characteristic imaging features, sometimes extending to involve enhancement of the cranial nerve surfaces (Box 3). *Meningitis* is the inflammation of the meninges; bacterial and viral meningitis commonly exhibit thin, linear leptomeningeal enhancement, whereas fungal and atypical bacterial meningitis display thicker, irregular, or nodular enhancement.[1,11] Carcinomatous meningitis related to meningeal spread of primary/secondary tumors also seems as enhancing leptomeningeal nodules, often with pachymeningeal enhancement.[1,12]

Meningitis comprises about 15% of all annual CNS infections; bacterial causes account for about two-thirds of such cases.[13] Clinical features in adults include a classic triad of fever, nuchal rigidity, and altered mental status. Kernig's sign (pain elicited by passive knee extension) and Brudzinski's sign (hip/knee flexion elicited by passive neck flexion) may also be present. Although these classic symptoms are not sensitive, they are highly specific. About 95% of adults hospitalized with community-acquired bacterial meningitis had greater than 2 of the 4 symptoms of headache, fever, neck stiffness, and altered sensorium, and 33% of adults had focal neurologic deficits.[14] Older adults may present with lethargy but without nuchal rigidity or fever, whereas children may experience irritability, vomiting, and even hydrocephalus (Box 4).[15] Dermatologic lesions such as maculopapular/petechial rashes may indicate meningococcal meningitis or endocarditis from staphylococci or pneumococci.[15,16]

In the clinical workup of suspected meningitis, CSF analysis by LP is a mainstay for diagnosing the pathogen and determining antimicrobial sensitivity. For bacterial meningitis, CSF analysis may reveal neutrophilic pleocytosis, elevated protein, and low glucose. Fungal meningitis has similar findings but often with very elevated opening pressure and normal glucose. Viral meningitis commonly presents as normal glucose with lymphocytic pleocytosis.[15] Although guidelines suggest that clinical features are deemed to be fairly accurate in predicting mass effect, many clinicians will still order CT before an LP for patients with suspected meningitis out of an abundance of caution.[16] Often, CT is preferred as the initial screening test for patients presenting with altered sensorium, focal neurologic deficits (besides cranial neuropathies), seizures, papilledema, vomiting, Cheyne-Stokes respirations or other signs of mass effect, and high intracranial pressure due to risk of herniation.[15,17] Additional factors favoring CT before LP include immunocompromised status and/or history of neurologic disorders. Imaging can also rule out meningitis mimics and elevated intracranial pressure before LP and assess for complications, such as edema and hydrocephalus.[1,15,18]

IMAGING OF MENINGITIS

Computed Tomography

Unenhanced CT can display mild dilatation of the ventricles with effaced subarachnoid spaces and suggestion of diffuse cerebral swelling. Obliteration of the normal basilar or convexity cisterns by exudates (of soft-tissue density) may also be seen (Fig. 9).[1] For older adults with large ventricles and effaced sulci/cisterns (as in ventriculo-sulcal discordance from normal pressure hydrocephalus), it may be necessary to consider acute conditions such as meningitis before labeling them with chronic diagnoses such as normal pressure hydrocephalus or age-related volume loss, in the appropriate clinical setting.

MR Imaging—Given its superior soft tissue contrast, MR imaging is much more sensitive at detecting meningitis and visualizing the soft tissue contrast in the basal cisterns, sylvian fissure, and sulcal regions. T1-weighted MR imaging may show obliteration of the basilar cisterns with enhancing inflammatory exudates (see Fig. 9H). Further, fluid attenuated inversion recovery (FLAIR) sulcal hyperintensities and leptomeningeal enhancement (see Figs. 8 and 9) may occur from elevated protein content in infectious exudates. FLAIR MR imaging is likely more sensitive than contrast enhancement in detecting leptomeningitis,[12] although the differential diagnosis is still broad (Box 5).[19]

Based on disease *chronicity*, meningeal enhancement of acute meningitis has a predilection for the cerebral convexity while chronic meningitis often involves the basilar cisterns. Enhancement in chronic meningitis is associated with dural thickening and sometimes popcornshaped dural calcifications.[1,20]

Diffusion-Weighted Imaging

Diffusion restriction is noted when there is increased DWI (b1000) signal and reduced ADC signal. DWI can demonstrate vascular complications such as infarcts from associated vasculitis,[1] meningeal and ependymal involvement in meningitis and ventriculitis,[21] and subtle, tiny amounts of restricted diffusion typically representing small collections of pus in the subarachnoid space and ventricles.[22]

CAUSES FOR INFECTIOUS MENINGITIS

Acute Pyogenic Meningitis

Acute pyogenic infections display diffuse leptomeningeal involvement and are more common in children. Purulent infections are often bacterial in origin, although enteroviruses can also cause acute meningitis. Frequent causes of bacterial infections are reviewed in Box 6. Immunocompromised patients may encounter *Pseudomonas, Klebsiella*, and fungal infections. Despite initiating empiric treatment, about 15% of patients experience neurologic complications and mortality remains around 20%.[1,15,20]

Acute Lymphocytic Meningitis

Acute lymphocytic meningitis from viral origin is generally benign and self-limited. History often includes travel, exposures, and new medications. Clinical signs are nonspecific,

such as headache, fever, and meningismus.[15] Pathogens involved include enteroviruses, HSV, and mumps. Imaging findings are often normal but may demonstrate subtle, thin, linear, leptomeningeal enhancement (with parenchymal enhancement if there is associated encephalitis).[1,20]

Eosinophilic Meningitis

Eosinophilic meningitides are rare disorders defined by the presence of 10 or more eosinophils per cubic millimeter in CSF or CSF eosinophilia greater than 10%. It is generally caused by helminthic parasites endemic to the tropics and contracted by ingestion of contaminated food (Box 7). For example, angiostrongyliasis is associated with ingestion of raw seafood or contaminated vegetables. CSF studies indicate a raised eosinophil count with normal glucose levels. MR imaging depicts prominent perivascular spaces, periventricular T2 hyperintensities and enhancing subcortical lesions. Proton magnetic resonance spectroscopy (^{1}H-MRS) may show reduced choline within lesions, associated with neuronal damage.[1] Diagnosis is confirmed by presence of antibodies against *Angiostrongylus*, etc.[23]

Recurrent and Mollaret Meningitis

Episodic, recurrent meningitis is often linked to streptococci and gram-negative bacilli and can be responsible for up to 16% of all meningitis events.[1] Mollaret meningitis (also called idiopathic recurrent meningitis), is a rare syndrome with recurring episodes of aseptic meningitis seen in young females and linked to HSV (HSV2>1). Episodes are associated with reactivation and positive CSF markers for HSV2 by polymerase chain reaction analysis.[24,25] Specific imaging features have yet to be described.[26]

CEREBRITIS AND INTRACRANIAL ABSCESS

Cerebritis is a region of poorly defined acute brain inflammation with increased permeability of local vessels but without neovascularization or angiogenesis.[11] Cerebritis can arise from pyogenic infections and inflammatory conditions and may progress to form an abscess if left untreated. A pyogenic *abscess* is a focal area of parenchymal infection consisting of a central cavity of purulent exudate and surrounding vascularized, collagenous capsule.[2,27] The pathophysiology of abscess involves spread by hematogenous dissemination, direct invasion, or iatrogenic complications. Similar to metastasis, hematogenous dissemination typically results in multiple abscesses near the gray–white junction within middle cerebral artery territories bilaterally. Children with abscess may have underlying congenital heart disease. Other infectious sources include pulmonary abscess and arteriovenous malformation, bacterial endocarditis, intra-abdominal abscess, and dental infection. Abscesses can be adjacent to untreated otitis media and odontogenic infections. Abscess from neurosurgical procedures is also increasing, related to higher procedure frequency.[2]

Intracranial abscess constitutes about 4% of all CNS infections annually.[13] Brain abscess is more prevalent in men than in women and more commonly occurs in the first 4 decades of life. Pre-disposing factors include diabetes, alcoholism, intravenous drug use, pulmonary lesions, and immunosuppression.[4]

Symptoms vary by abscess location, extent of mass effect, and associated complications. Developing abscesses result in neurologic symptoms[15] (Box 8) that overlap with meningitis including headache (50%–90%), fever (60%), and altered sensorium (30%–70%). Abscesses with high intracranial pressure may present with papilledema. Laboratory tests are often unrevealing; indeed, the absence of leukocytosis or pathogens in the CSF does not preclude the diagnosis of abscess.[4] LP is often discouraged and even contraindicated in order to avoid herniation or ventricular rupture when neuroimaging demonstrates surrounding edema, mass effect, or increased intracranial pressure.[15] Blood cultures may reveal the underlying cause of abscess in the setting of hematogenous dissemination, although direct aspiration is often required for establishing accurate diagnosis and subsequent treatment.

IMAGING OF CEREBRITIS AND ABSCESS

The advent of CT and MR imaging has enabled rapid localization, accurate diagnosis, stereotactic aspiration, and serial postoperative evaluation of abscesses while improved newer generation antibiotics have enabled better empiric and selective therapy.[2,27] There should be a low threshold for performing neuroimaging when complications of meningitis are suspected and treatment planning can be further clarified. Intracranial abscesses greater than 1 cm are stereotactically aspirated while patients are on broad-spectrum antimicrobials and steroids.[28,29] Careful consideration is needed before biopsy of presumed cerebritis. Follow-up imaging is performed if there is clinical decline, a lack of improvement after 1 to 2 weeks and after recovery.[29]

Meningitis with Cerebritis and Abscess

Meningitis is accompanied by abscess in about 2% of patients with CNS infection. There are 3 common scenarios: (1) community-acquired bacterial meningitis can be complicated by cerebritis and abscess, (2) patients with infective endocarditis concurrently develop meningitis and focal abscess via mycotic emboli, and (3) abscess capsules rupture causing ependymal/meningeal spread and sudden decline.[2,30]

Computed Tomography

CT with contrast can evaluate the 4 stages of pyogenic infection: early cerebritis, late cerebritis, early capsule formation, and mature abscess.[30,31] In early cerebritis, bacteria enter the parenchyma, triggering an immune response resulting in perivascular swelling. On CT, this is seen as an ill-defined low attenuation with variable contrast enhancement. In late cerebritis, central necrosis is flanked by stromal matrix, leading to low attenuation with rim enhancement that is stable on delayed images. During full abscess formation stages, a collagenous surrounding capsule forms, appearing as ring enhancement that decays on delayed images (which corresponds to granulation tissue). Because the medial or ventricular wall of an abscess is thinner than the lateral wall, due to the blood supply gradient, an untreated abscess near the ventricles often ruptures, causing satellite abscesses and ventriculitis.[2,31]

MR Imaging

As with meningitis, abscess is better diagnosed with MR imaging compared with CT, especially due to sensitivity of MR imaging to water diffusion. Moreover, MR imaging is vital to the longitudinal evaluation of abscess. Cerebritis shows nonspecific, ill-defined T2/FLAIR hyperintensity and mild T1 hypointensity with poorly demarcated enhancement. In contrast, mature abscesses show central low intensity on T1 and central high intensity on T2 with surrounding vasogenic edema.[2,20] Most importantly, abscesses are a canonical *ring enhancing* lesion. On postcontrast T1-weighted MR imaging, the capsule seems as an enhancing, smooth, thin, circumferential rim that is T1 hyperintense and T2 hypointense relative to white matter (see Fig. 8; Fig. 10).[2] In fact, the T2 hypointense abscess capsule may seem as a "dual rim sign" of concentric circles (either complete or incomplete), which is a useful imaging clue to distinguish from necrotic gliomas (see Fig. 10).[32] The differential diagnosis for ring enhancement is described further in the "Mimics" section.

Diffusion-Weighted Imaging—Central diffusion restriction is a hallmark feature of most forms of untreated abscess, due to proteinaceous contents of inflammatory exudates/pus,[22] with high signal on DWI maps and low signal on ADC maps (see Fig. 10). Athough cerebritis does not contain frank pus and often does not exhibit diffusion restriction (see Fig. 3), abscess does restrict water diffusion, reflecting the inflammatory milieu of necrotic debris, highly viscous proteinaceous exudates, and viable bacterial and immune cells in abscess cavities. Conversely, the central nonenhancing regions of a peripherally enhancing necrotic high-grade glioma contain fewer inflammatory cells and less viscous, clearer serous fluid that shows facilitated diffusion. Hence, DWI can accurately distinguish abscess from necrotic gliomas.[1,2,29] Although most bacterial abscesses seem centrally diffusion restricting,[33] other ring-enhancing entities such as toxoplasmosis may lack this critical finding.[34,35]

Quantification of ADC values can further assist in the differential diagnosis of enhancing mass lesions. Compared with cerebral white matter, which has a mean ADC value near 0.9×10^{-3} mm^2/s,[36] pyogenic abscesses usually have mean ADC values 30% to 40% lower, at 0.5 to 0.6×10^{-3} mm^2/s.[37,38] Compared with the low mean ADC values of spontaneous brain abscesses,[37,38] other mass lesions often have mean ADC values higher than 1.3×10^{-3} mm^2/s, including gliomas,[37–39] toxoplasmosis,[39] and iatrogenic postoperative brain abscesses.[40] Nevertheless, diffusion restriction in abscess often become less prominent on treatment initiation and may help distinguish between therapeutic success and the reaccumulation of infectious material/pus.[38]

MR Spectroscopy

Mature brain abscesses have certain spectroscopic profiles that distinguish them from neoplasms on ^{1}H-MRS (Box 9). Although abscess and tumors share features such as decreased normal neuronal metabolites, choline (3.2 ppm) is elevated in brain tumors and can be used to distinguish from pyogenic abscess (Fig. 11). In addition, pyogenic abscesses demonstrate signal from cytosolic, branched chain amino acids (valine, leucine, isoleucine, 0.9 ppm) and succinate (2.4 ppm), which diminish on successful therapy.[2] Because acetate is a product and substrate in anaerobic bacterial metabolism,[41] elevated acetate peaks

(1.9 ppm) are also often present in anaerobic abscesses (Fig. 12).[2,42,43] Although these are general MRS findings typically associated with abscess, exceptions exist.[44] Overall, ^{1}H-MRS is more supportive than determinative and has 72% to 100% sensitivity and 30% to 100% specificity.[45,46]

In immunocompromised patients, ^{1}H-MRS can assist in distinguishing toxoplasmosis from primary CNS lymphoma. The increase in lipid and lactate peaks (1.3 ppm) is usually much more substantial in toxoplasmosis than lymphoma while the increase of choline (3.2 PM) is higher in lymphoma and often decreased in toxoplasmosis.[46]

Nuclear Medicine

Focal intracranial infections can also be evaluated using metabolic PET tracers, although this is not widely used in clinical practice. Although ^{18}F-fluorodeoxyglucose (^{18}F-FDG) uptake can detect hypermetabolism associated with infections such as rhinocerebral mucormycosis,[47] infections generally have less metabolic activity than tumors. When differentiating lymphoma from toxoplasmosis in patients with human immunodeficiency virus (HIV), note that lymphoma exhibits significant uptake of radiotracers in ^{18}F-FDG PET and ^{201}Th and ^{99m}Tc-sestamibi single-photon emission CT. These tracers also have ~100% sensitivity and 60% to 90% specificity in identifying lymphoma over toxoplasmosis.[48,49]

Artificial Intelligence for Central Nervous System Infections

With the increasing adoption of deep learning in medicine, AI models have demonstrated remarkable accuracy and efficiency on an assortment of neuroimaging tasks and disease-specific applications.[50–54] For instance, neural networks could distinguish between bacterial and viral meningitis.[55] Recent convolutional neural networks (such as U-Net) can perform at the level of radiologists on FLAIR lesion detection.[56] Moreover, the integration of these deep learning models with Bayesian inference enables accurate and interpretable probabilistic differential diagnoses for an array of CNS infections (including abscess, toxoplasmosis, cryptococcosis) and their mimics[57] as well as HIV encephalopathy and progressive multifocal leukoencephalopathy.[58] Because neural networks can identify and predict signature imaging findings in cerebral infections, including ring enhancement and FLAIR hyperintensities,[59] clinical validation and integration studies are the next phase in translating this research into augmenting the radiologist's workflow in the future (Fig. 13).

CAUSES FOR CEREBRITIS, ABSCESS, AND CEREBRAL INVOLVEMENT

Bacterial Abscess

Most intracranial abscesses are polymicrobial in composition, including aerobic and/or anaerobic bacteria (Box 10). Immunocompetent patients may develop bacterial abscesses due to infective endocarditis, pulmonary shunts, trauma, and dental/sinus infections,[28] whereas immunocompromised patients typically present with fungal and *Nocardia* abscesses.[15] Note that abscess in immunocompromised patients may not display the typical ring enhancement, restricted diffusion, and/or vasogenic edema, and the lack of inflammatory response is usually associated with worse outcomes.[2]

Aspergillosis

Cerebral aspergillosis is a common cause of abscess in immunocompromised cohorts with a mortality of about 90%.[60] Along with candidiasis, aspergillosis is one of the most common sources of intracranial fungal abscess (aspergilloma) and arises in the settings of neutropenia, transplantation, and HIV infection.[20,29] Aspergillomas are usually ring enhancing and T1 hypointense with central diffusion restriction on DWI.[33,61] Angioinvasive aspergillosis tends to infiltrate and occlude smaller perforating vessels supplying the basal ganglia, thalami, corpus callosum, and brainstem. Because hemorrhage occurs in 25% of aspergillomas and even more commonly in invasive aspergillosis, ferromagnetic blood products in such lesions might seem T1 hyperintense and susceptible on gradient echo (GRE) sequence (Fig. 14).[61] *Aspergillus* meningitis rarely occurs in immunocompetent individuals.[60]

Nocardiosis

Nocardia is a branching, filamentous bacteria that is weakly acid fast, distinguishing it from *Actinomyces* on staining. Although *Actinomyces* is linked to odontogenic abscess, nocardiosis is related to HIV infection and immunosuppression.[29] Importantly, pulmonary nocardiosis in immunocompromised patients should undergo screening intracranial imaging.[15] Compared with other causes, nocardial abscess is usually multiloculated (Fig. 15).[62]

Toxoplasmosis

Toxoplasmosis is caused by *Toxoplasma gondii*. It is the most frequent opportunistic infection linked to HIV and occurs in 33% of patients with HIV,[34] toxoplasmosis lesions often seem as multifocal nodules in the basal ganglia or frontoparietal regions (Fig. 16A–C), with disproportionate extent of vasogenic edema and/or hemorrhage and without periventricular spread typically seen in lymphoma.[1,47] Differences may be noted on MRS[46] and ^{18}F-FDG PET.[48] Although the “eccentric target sign” for cerebral toxoplasmosis only has 25% sensitivity and is seen in only 30% of cases, it is greater than 95% specific.[63] The eccentric target sign is seen on postcontrast images as irregular ring enhancement with eccentric nodularity, likely from invagination of the abscess wall with inflamed vessels in its groove, surrounded by perilesional edema, inflammation, and demyelination.[64] Although abscess and toxoplasmosis both have peripheral enhancement, the central diffusion restriction seen in abscess is generally absent in toxoplasmosis (Fig. 16D, E).[34] Compared with parenchymal infection, toxoplasma meningitis is rare in HIV infection or transplant recipients,[65] and cryptococcal/tuberculous meningitis and lymphoma should be considered in the differential diagnosis of abnormal meningeal enhancement.[66]

CAUSES WITH MIXED MENINGEAL AND CEREBRAL INVOLVEMENT

Chronic Meningitis and Abscess: Tuberculosis and Cryptococcosis

Exudates from chronic meningitides (tubercular or fungal) seem as thick, nodular leptomeningeal enhancement and often coalesce into localized forms of infection such as tuberculoma, cryptococcoma, and so forth.[20]

Tuberculous meningitis occurs through hematogenous dissemination. CSF findings are often nonspecific and only show the pathogen in about 30% of cases.[15,67] On imaging, tuberculous meningitis displays basal and posterior fossa leptomeningeal enhancement associated with hydrocephalus. Vasculitis, thrombosis, and infarction may also be seen (Fig. 17).[68,69] Tuberculomas are ring-enhancing lesions that are heterogeneously T2 hypointense.[70] Unlike typical abscesses, tuberculomas usually do not exhibit central diffusion restriction due to caseous necrosis, although the periphery may.[35] On ^{1}H-MRS, tuberculomas exhibit elevated lipid peaks (1.3 ppm), derived from mycolic acid, yet lack cytosolic amino acids (0.9 ppm).[2,20]

Cryptococcosis has a predilection for the neuraxis in immunocompromised patients.[1,20] On contrast-enhanced MR imaging, cryptococcosis results in enhancement of the leptomeninges and perivascular spaces (Fig. 18). Parenchymal lesions frequently occur around the basal ganglia and include ring-enhancing cryptococcomas and diffusion-restricting gelatinous pseudocysts that are associated with edema and infarcts. The gelatinous pseudocysts represent spread of the fungi via perivascular spaces, leading to dilation and enhancement of these pial-lined, fluid-filled structures.[71] Serial LP, ventriculoperitoneal shunts and steroids mitigate elevated intracranial pressures, hydrocephalus and edema.[72] Immunocompromised patients have worse outcomes and may not present with edema and enhancement.[73]

Neurocysticercosis

Neurocysticercosis is the most prevalent CNS infection worldwide, accounting for 83% of all CNS infections annually. It is endemic in Asia, Africa and Latin America, where it is the commonest cause of seizures and CSF eosinophilia.[13] There are 3 types of disease: meningobasilar (most common), ventricular and parenchymal.[74] About 60% of patients also demonstrate parenchymal cysts.[75,76] There are 4 classic stages of disease. In the early vesicular stage of parenchymal cysticercosis, cysts often manifest as a “dot in a hole” attributed to a visible scolex or hooked mouth of the parasite inside the lesion (Fig. 19). The scolex inner “dot” seems T2 hypointense, FLAIR hyperintense, and enhancing[76] and may be well visualized on 3D constructive interference in steady state MR sequence (see Fig. 19B).[77] This stage is followed by the vesicular-colloidal, granular nodular, and calcified nodular stages. As the parasite dies, the cyst ruptures, recruiting inflammatory cells with edema, altering signal intensity and ultimately causing calcification.[1,20]

OTHER COMPLICATIONS OF MENINGITIS, CEREBRITIS, AND ABSCESS

Ventriculitis

Ventriculitis (or ependymitis) is the involvement of the ependyma, choroid plexus, and/or ventricles and is a very severe complication that occurs in 30% of patients with CNS infections. Organisms such as *Staphylococcus aureus* and *Enterobacter* can breach the ventricular system via (1) direct extension from trauma or neurosurgical intervention, (2) meningeal spread into the ventricles, (3) hematogenous dissemination through the subependyma and choroid plexus, (4) CSF backflow from extraventicular to intraventricular spaces, and (5) abscess rupture. Clinical progression is insidious, so it is paramount to treat the underlying source assiduously.[1,15]

Chronic viral infections can produce periventricular calcifications.[7] Cranial ultrasound in children is often superior to CT and may reveal irregular, echogenic ependyma, intraventricular debris, and stranding associated with ventricular dilatation.[1] MR imaging is most revealing; the ependyma enhances while the ventricles are dilated and filled with T2/FLAIR hyperintense, diffusion restricting purulent exudate (see Fig. 2; Fig. 20). Notably, higher ADC values might be observed from mixing of CSF and pus.[7,21]

Hydrocephalus and Herniation

Hydrocephalus in CNS infections varies from mild/transient (81% of cases) to severe (5%),[78,79] which can lead to brain herniation and sudden death (see Fig. 9). Hydrocephalus arises when (1) debris impedes CSF resorption, (2) infections infiltrate the ventricular system, or (3) mass lesions compress drainage structures.[79] Moreover, ruptured cysticercal scolex lesions and mycobacterial antigens are immunogenic in 30%[80] and 65% of cases, respectively.[69] Hydrocephalus also occurs in up to 60% of patients with cryptococcosis and is associated with very-high LP opening pressures (>350 mm H_2O in 50% of cases; Fig. 21). Large abscesses create inflammatory exudate, vasogenic edema and mass effect, midline shift, and herniation. In cryptococcosis, CSF shunting or sequential LP can prevent herniation.[72]

Extra-Axial Collections

Extra-axial fluid collections associated with infections can be sterile (effusion) or purulent (empyema). Microbes can induce inflammation of the dura and subdural veins, creating subdural effusions. Most sterile effusions seem along the frontal and temporal convexities and tend to resolve spontaneously within months. If such findings produce mass effect, drainage may be warranted.[7] Typically, imaging of subdural effusions reveals crescentic collections of similar density/intensity as CSF. Some effusions may resemble empyema after accruing fibrin deposits and proteinaceous collections, possibly demonstrating enhancement on postcontrast MR imaging and failure of FLAIR suppression.[81,82] Presence of diffusion restriction, however, favors empyema over effusion.[83]

Empyemas are life-threatening and should be drained. Streptococci are the most common pathogens, followed by *S aureus* and anaerobes. The clinical presentation is more severe and persistent than effusion.[15] Subdural empyema is located between the dura and arachnoid mater over the convexities or between hemispheres (Fig. 22). It is often due to thrombophlebitis from emissary veins. CT depicts a hypodense/isodense crescentic or lenticular collection while MR imaging shows a diffusion restricting crescentic collection with surrounding enhancement.[7] Perilesional T2/FLAIR hyperintensities of the cortex and concomitant venous thrombosis and infarct are specific to empyema compared with effusions. Epidural empyema seems between the dura and calvaria and is more insidious and benign. Similar to subdural empyema, epidural empyema has FLAIR hyperintensities but is biconvex in shape (Fig. 23) and may occasionally have low/mixed DWI signal as the pus is less viscous and inflammatory.[81]

Cranial Nerve Involvement

Cranial nerve enhancement is almost always pathologic. Differential diagnosis includes infection, inflammation, demyelination, toxicmetabolic, genetic, neoplastic, and idiopathic (ie, Tolosa-Hunt syndrome, Fig. 7).[84] Basal meningeal exudates can cause compression, strain, and ischemia of cranial nerves, leading to diplopia, facial palsy, hearing loss, and so forth (Fig. 24). Meningitis associated with otitis media from *Streptococcus pneumoniae*, *Haemophilus influenza*, and *Neisseria meningitidis* can result in transient and permanent sensorineural hearing loss in 15% to 30% of cases.[85,86] Local involvement such as labyrinthitis with inner ear sclerosis may be visualized on CT and T2-weighted MR imaging. Note that meningitis-induced hearing loss should be differentiated from hearing loss secondary to ototoxic antibiotics.[7] Additional cranial neuropathies impair the optic, oculomotor, and facial nerves. Cranial neuropathy may seem as cranial nerve and perineural enhancement and classically presents in neuroborreliosis, tuberculous meningitis, cryptococcosis, and schistosomiasis.[84]

Venous Sinus Thrombosis, Vasculitis, and Infarction

Venous sinus thrombosis occurs in 1% of patients with meningitis·[87] Cerebral venous thrombosis can evolve into infarct in 30% of patients.[7] Venous sinus thrombosis can also develop secondary to bacterial meningitis, pyogenic infection (see Fig. 3; Fig. 25) and mastoiditis.

Infectious vasculitis can complicate syphilis, tuberculous meningitis (Fig. 26), angioinvasive aspergillosis and other infections. Ischemic strokes associated with vasculitis occur in 14% of patients with neurosyphilis.[88]

Infarction occurs in up to 30% of adults with bacterial meningitis,[89] especially chronic meningitis: 13% to 32% of patients with cryptococcal meningitis[90,91] (see Fig. 18) and about 25% to 40% of patients with tuberculous meningitis.[92,93] Tuberculosis-associated infarcts predominantly localize to the basal ganglia and thalamus, which are supplied by small Circle of Willis branches including the medial lenticulostriate and thalamoperforating arteries, as well as lateral lenticulostriate, anterior choroidal, and thalamogeniculate arteries,[94] although the exact frequencies are debated.[92] Hence, the risk of infarct in tuberculous meningitis is more correlated with the presence of basal meningeal enhancement and vasospasm and less with the encapsulation of mycobacteria in a tuberculoma.[68,95]

MIMICS OF CENTRAL NERVOUS SYSTEM INFECTION

Radiographic features associated with CNS infections, such as meningeal or ring enhancement, are shared with many noninfectious disorders (see Box 1).

Meningeal Enhancement in Chemical/DrugInduced Meningitis

In particular, subacute noninfectious meningeal inflammation can share symptoms with infectious meningitis. Chemical meningitis occurs in response to nonmicrobial irritants in the subarachnoid space (blood, dermoid cyst rupture, intrathecal drug instillation), often in the setting of neurosurgery or neurointervention. CSF reveals leukocytosis, elevated protein,

and low glucose but negative cultures.[96] Drug-induced meningitis is rarely associated with certain nonsteroidal anti-inflammatory drugs (NSAIDs), intravenous immunoglobulin (IV-IG), and other therapies (Box 11). MR imaging findings are nonspecific, including pial and dural enhancement. Immunotherapy-induced meningitis may resemble infectious or carcinomatous meningitis.[97] Symptoms and CSF pleocytosis resolve quickly on drug withdrawal.[98]

Meningeal Enhancement in Neoplasia

Leptomeningeal enhancement or *carcinomatous meningitis* is the spread of neoplasm across the subarachnoid space (Fig. 27). Timely imaging and diagnosis are critical because carcinomatous meningitis is a marker of advanced disease and the median survival time without treatment is about 4 to 6 weeks. Metastases, lymphoma, and primary CNS tumors impair the BBB and promote contrast leakage, typically appearing as nodular leptomeningeal enhancement.[97] Some tumors are also associated with focal pachymeningeal enhancement. Meningioma tumor cells recruit blood vessels, promoting vasocongestion and interstitial edema resulting in thickened dura, pachymeningeal enhancement and the classic “dural tail sign.”[99] Schwannomas can show perineural meningeal enhancement.[11] Meningeal involvement in paraneoplastic limbic encephalitis is reported but uncommon (<10%).[100]

Meningeal Enhancement in Neurosarcoidosis

Neurosarcoidosis is an archetypal neuroinflammatory granulomatous disease with a predilection for meningeal enhancement. It occurs in about 10% of patients with sarcoidosis. Granulomatous basal leptomeningitis, ependymitis, and inflammation of the perivascular spaces can result in edema, causing headache, nuchal rigidity, cranial neuropathy, visual symptoms, and motor weakness. Given the variable presentation of neurosarcoidosis, diagnosis requires a high degree of clinical suspicion.[15] Hallmark basal meningeal enhancement can be focal or diffuse with nodular leptomeningeal or pachymeningeal enhancement.[100,101] Enhancement of the pituitary stalk, cranial nerves, and perivascular spaces with white matter changes and hydrocephalus can occur (Fig. 28). Enhancement coincides with lesion activity and generally improves with steroid therapy.[102] Systemic involvement with ^{18}F-FDG avid nodules of the lungs, heart, lymph nodes, and skin are highly supportive of neurosarcoidosis.[103] Additional causes of neuroinflammatory conditions include posterior reversible encephalopathy syndrome and chronic lymphocytic inflammation with pontine perivascular enhancement responsive to steroids.[104,105]

Ring-Enhancing Lesions

Ring-like contrast enhancement is a sensitive though nonspecific radiologic feature for intracranial abscess (Box 12, Fig. 29). In a series of 221 ring-enhancing lesions, the most frequent diseases were glioma (40%), followed by metastasis (30%), abscess (8%), and multiple sclerosis (6%).[106] Tumors tend to be solitary, necrotic lesions, whereas abscess and demyelinating lesions were more often multifocal. In immunocompromised patients, diseases that traditionally seem as single masses, such as primary CNS lymphoma, may manifest as multifocal ring-enhancing lesions (Fig. 29).[107] Demyelinating lesions generally exhibit incomplete ring enhancement. Abscesses generally elicit a greater foreign

immune response and edema, with smooth, circumferential capsules with central diffusion restriction.[2,11,108]

SUMMARY

Numerous infectious and noninfectious conditions share enhancement and diffusion restriction patterns in the meninges and brain parenchyma. Therefore, a solid foundation of anatomy, pathophysiology, and clinical medicine guides appropriate neuroimaging interpretation of meningitis, abscess, and their mimics. CT, MR imaging, DWI, MRS, PET, and other imaging modalities support the diagnosis, treatment planning, and monitoring for CNS infections. Newer imaging methods and deep learning algorithms may improve diagnostic imaging capacity. Overall, the integration of neuroimaging with clinical history and laboratory results is vital for suitable CNS infection workup and management.

DISCLOSURE

S. Mohan has grant funding from the National Cancer Institute (NCI R01 CA262584), Galileo CDS and Novocure, USA. M. T. Duong has research funding from the National Institute on Aging (NIA F30 AG074524). J. D. Rudie has research support from the National Institute of Biomedical Imaging and Bioengineering (NIBIB T32 EB004311) and Radiological Society of North America (RSNA RR1778) research grant. There are no additional disclosures to report.

REFERENCES

1. Mohan S, Jain KK, Arabi M, et al. Imaging of Meningitis and Ventriculitis. Neuroimaging Clin N Am 2012;22(4):557–83. [PubMed: 23122257]
2. Rath TJ, Hughes M, Arabi M, et al. Imaging of Cerebritis, Encephalitis, and Brain Abscess. Neuroimaging Clin N Am 2012;22(4):585–607. [PubMed: 23122258]
3. Global Burden of Disease 2016 Meningitis Collaborators. Global, regional, and national burden of meningitis, 1990–2016: a systematic analysis for the Global Burden of Disease Study 2016. Lancet Neurol 2018;17(12):1061–82. [PubMed: 30507391]
4. Patel K, Clifford DB. Bacterial Brain Abscess. Neurohospitalist 2014;4(4):196–204. [PubMed: 25360205]
5. Mortazavi MM, Tubbs RS, Riech S, et al. Anatomy and pathology of the cranial emissary veins: a review with surgical implications. Neurosurgery 2012;70(5):1312–8. [PubMed: 22127046]
6. Absinta M, Ha S-K, Nair G, et al. Human and nonhuman primate meninges harbor lymphatic vessels that can be visualized noninvasively by MRI. eLife 2017;6:e29738. [PubMed: 28971799]
7. Castillo M Imaging of meningitis. Semin Roentgenol 2004;39(4):458–64. [PubMed: 15526529]
8. Montagne A, Toga AW, Zlokovic BV. Blood-brain Barrier Permeability and Gadolinium: Benefits and Potential Pitfalls in Research. JAMA Neurol 2016;73(1):13–4. [PubMed: 26524294]
9. Wesley SF, Garcia-Santibanez R, Liang J, et al. Incidence of meningeal enhancement on brain MRI secondary to lumbar puncture. Neurol Clin Pract 2016;6(4):315–20. [PubMed: 29443119]
10. Mokri B The Monro-Kellie hypothesis: applications in CSF volume depletion. Neurology 2001;56(12):1746–8. [PubMed: 11425944]
11. Smirniotopoulos JG, Murphy FM, Rushing EJ, et al. Patterns of Contrast Enhancement in the Brain and Meninges. RadioGraphics 2007;27:551–626.
12. Koksel Y, McKinney AM. Potentially Reversible and Recognizable Acute Encephalopathic Syndromes: Disease Categorization and MRI Appearances. AJNR Am J Neuroradiol 2020. 10.3174/ajnr.A6634.
13. Robertson FC, Lepard JR, Mekary RA, et al. Epidemiology of central nervous system infectious diseases: a meta-analysis and systematic review with implications for neurosurgeons worldwide. J Neurosurg 2018;130(4):1039–408.

14. van de Beek D, de Gans J, Spanjaard L, et al. Clinical features and prognostic factors in adults with bacterial meningitis. N Engl J Med 2004;351(18):1849–59. [PubMed: 15509818]
15. Srinivasan J, Chaves CJ, Scott BJ, et al. Netter's Neurology. 3rd ed. Philadelphia: Elsevier; 2020.
16. van de Beek D, Cabellos C, Dzupova O, et al. ESCMID guideline: diagnosis and treatment of acute bacterial meningitis. Clin Microbiol Infect 2016;22:S37–62. [PubMed: 27062097]
17. Hasbun R, Abrahams J, Jekel J, et al. Computed tomography of the head before lumbar puncture in adults with suspected meningitis. N Engl J Med 2001;345(24):L1727–33.
18. Salazar L, Hasbun R. Cranial Imaging Before Lumbar Puncture in Adults With Community-Acquired Meningitis: Clinical Utility and Adherence to the Infectious Diseases Society of America Guidelines. Clin Infect Dis 2017;64(12):1657–62. [PubMed: 28369295]
19. Shang WJ, Shu CLM, Liao HW, et al. The Association between FLAIR Vascular Hyperintensity and Stroke Outcome Varies with Time from Onset. AJNR Am J Neuroradiol 2019;40:1317–22. [PubMed: 31371355]
20. Shih RY, Koeller KK. Bacterial, Fungal, and Parasitic Infections of the Central Nervous System: Radiologic-Pathologic Correlation and Historical Perspectives. Radiographics 2015;35(5):1141–69. [PubMed: 26065933]
21. Pezzullo JA, Tung GA, Mudigonda S, et al. Diffusion-Weighted MR Imaging of Pyogenic Ventriculitis. AJR Am J Roentgenol 2003;180:71–5. [PubMed: 12490479]
22. Tung GA, Rogg JM. Diffusion-weighted imaging of cerebritis. AJNR Am J Neuroradiol 2003;24(6):1110–3. [PubMed: 12812934]
23. Senthong V, Chindaprasirt J, Sawanyawisuth K. Differential Diagnosis of CNS Angiostrongyliasis: A Short Review. Hawaii J Med Public Health 2013;72:52–4. [PubMed: 23901385]
24. Shalabi M, Whitley RJ. Recurrent Benign Lymphocytic Meningitis. Clin Infect Dis 2006;43(9):1194–7. [PubMed: 17029141]
25. Min Z, Baddley JW. Mollaret's meningitis. Lancet Infect Dis 2014;14:1022. 10.1016/S1473-3099(14)70874-6. [PubMed: 25253408]
26. Prandota J Mollaret meningitis may be caused by reactivation of latent cerebral toxoplasmosis. Int J Neurosci 2009;119(10):1655–92. [PubMed: 19922380]
27. Villanueva-Meyer JE, Cha S. From Shades of Gray to Microbiologic Imaging: A Historical Review of Brain Abscess Imaging. RadioGraphics 2015;35:1555–62. [PubMed: 26207582]
28. Sonneville R, Ruimy R, Benzonana N, et al. An update on bacterial brain abscess in immunocompetent patients. Clin Microbiol Infect 2017;23(9):614–20. [PubMed: 28501669]
29. Brouwer MC, Tunkel AR, McKhann GM, et al. Brain Abscess. N Engl J Med 2014;371:447–56. [PubMed: 25075836]
30. Jim KK, Brouwer MC, van der Ende A, et al. Cerebral abscesses in patients with bacterial meningitis. J Infect 2012;64:236–8. [PubMed: 22120596]
31. Britt RH, Enzmann DR, Yeager AS. Neuropathological and computerized tomographic findings in experimental brain abscess. J Neurosurg 1981;55(4):590–603. [PubMed: 6168748]
32. Toh CH, Wei K-C, Chang C-N, et al. Differentiation of pyogenic brain abscesses from necrotic glioblastomas with use of susceptibility-weighted imaging. AJNR Am J Neuroradiol 2012;33(8):1534–8. [PubMed: 22422181]
33. Gaviani P, Schwartz RB, Hedley-Whyte E, et al. Diffusion-Weighted Imaging of Fungal Cerebral Infection. AJNR Am J Neuroradiol 2005;26(5):1115–21. [PubMed: 15891169]
34. Lee GT, Antelo F, Mlikotic AA. Cerebral Toxoplasmosis. RadioGraphics 2009;29(4):1200–5. [PubMed: 19605667]
35. Shetty B, Balla S, Reddy S. Radiological Society of North America 2005 Scientific Assembly and Annual Meeting, November 27 – December 2, 2005, Chicago IL. http://archive.rsna.org/2005/4418443.html.
36. Sener RN. Diffusion MRI: apparent diffusion coefficient (ADC) values in the normal brain and a classification of brain disorders based on ADC values. Comput Med Imaging Graph 2001;25(4):299–326. [PubMed: 11356324]

37. Guzman R, Barth A, Lövblad K-O, et al. Use of diffusion-weighted magnetic resonance imaging in differentiating purulent brain processes from cystic brain tumors. J Neurosurg 2002;97(5). 10.3171/jns.2002.97.5.1101.
38. Cartes-Zumelzu FW, Stavrou I, Castillo M, et al. Diffusion-Weighted Imaging in the Assessment of Brain Abscesses Therapy. Am J Neuroradiol AJNR 2004;25(8):1310–7. [PubMed: 15466324]
39. Chang SC, Lai PH, Chen WL, et al. Diffusion-weighted MRI features of brain abscess and cystic or necrotic brain tumors: comparison with conventional MRI. Clin Imaging 2002;26:227–36. [PubMed: 12140151]
40. Lotan E, Hoffmann C, Fardman A, et al. Postoperative versus Spontaneous Intracranial Abscess: Diagnostic Value of the Apparent Diffusion Coefficient for Accurate Assessment. Radiology 2016;281(1):168–74. [PubMed: 27027334]
41. Diekert G CO2 reduction to acetate in anaerobic bacteria. FEMS Microbiol Rev 1990;7(3–4): 391–5. 10.1111/j.1574-6968.1990.tb04942.x.
42. Pal D, Bhattacharyya A, Husain M, et al. In Vivo Proton MR Spectroscopy Evaluation of Pyogenic Brain Abscesses: A Report of 194 Cases. AJNR Am J Neuroradiol 2010;31(2):360–6. [PubMed: 19797788]
43. Öz G, Alger JR, Barker PB, et al. Clinical Proton MR Spectroscopy in Central Nervous System Disorders. Radiology 2014;270(3):658–79. [PubMed: 24568703]
44. Verma A, Kumar I, Verma N, et al. Magnetic resonance spectroscopy — Revisiting the biochemical and molecular milieu of brain tumors. BBA Clin 2016;5:170–8. [PubMed: 27158592]
45. Hsu S-H, Chou M-C, Ko C-W, et al. Proton MR spectroscopy in patients with pyogenic brain abscess: MR spectroscopic imaging versus single-voxel spectroscopy. Eur J Radiol 2013;82(8):1299–307. [PubMed: 23453705]
46. Chang L, Cornford ME, Chiang FL, et al. Radiologic-Pathologic Correlation: Cerebral Toxoplasmosis and Lymphoma in AIDS. AJNR Am J Neuroradiol 1995;16:1653–63. [PubMed: 7502971]
47. Sharma P, Mukherjee A, Karunithi S, et al. Potential Role of ^{18}F-FDG PET/CT in Patients With Fungal Infections. AJR Am J Roentgenol 2014;203:180–9. [PubMed: 24951213]
48. Marcus C, Feizi P, Hogg J, et al. Imaging in Differentiating Cerebral Toxoplasmosis and Primary CNS Lymphoma With Special Focus on FDG PET/CT. AJR Am J Roentgenol 2021;216(1):157–64. [PubMed: 33112669]
49. El Omri H, Hascsi Z, Taha R, et al. Tubercular Meningitis and Lymphadenitis Mimicking a Relapse of Burkitt's Lymphoma on 18F-FDG-PET/CT: A Case Report. Case Rep Oncol 2015;8:226–32. [PubMed: 26078742]
50. Zaharchuk G, Gong E, Wintermark M, et al. Deep Learning in Neuroradiology. AJNR Am J Neuroradiol 2018;39(10):1776–84. [PubMed: 29419402]
51. Rudie JD, Rauschecker AM, Bryan RN, et al. Emerging Applications of Artificial Intelligence in Neuro-Oncology. Radiology 2019;290:607–18. [PubMed: 30667332]
52. Rudie JD, Duda J, Duong MT, et al. Brain MRI Deep Learning and Bayesian Inference System Augments Radiology Resident Performance. J Digit Imaging 2021;34:1049–58. [PubMed: 34131794]
53. Duong MT, Rauschecker AM, Mohan S. Diverse Applications of Artificial Intelligence in Neuroradiology. Neuroimaging Clin N Am 2020;30(4):505–16. [PubMed: 33039000]
54. Duong MT, Rauschecker AM, Rudie JD, et al. Artificial intelligence for precision education in radiology. Br J Radiol 2019;92(1103):20190389. [PubMed: 31322909]
55. Ene M, Gorunescu M, Gorunescu F, et al. A Machine Learning Approach to Differentiating Bacterial From Viral Meningitis. IEEE John Vincent Atanasoff Int Symp Mod Comput 2006;155–62.
56. Duong MT, Rudie JD, Wang J, et al. Convolutional neural network for automated FLAIR lesion segmentation on clinical brain MR imaging. AJNR Am J Neuroradiol 2019;40(8):1282–90. [PubMed: 31345943]
57. Rudie JD, Rauschecker AM, Xie L, et al. Subspecialty-level deep gray matter differential diagnoses with deep learning and Bayesian networks on clinical brain MRI: a pilot study. Radiol Artif Intelligence 2020;2(5):e190146. 10.1148/ryai.2020190146.

58. Rauschecker AM, Rudie JD, Xie L, et al. Artificial Intelligence System Approaching Neuroradiologistlevel Differential Diagnosis Accuracy at Brain MRI. Radiology 2020;295(3):626–37. [PubMed: 32255417]
59. Rudie JD, Colby JB, Laguna B, et al. Automated Detection and Segmentation of Abnormal Enhancement Across 15 Neurological Diseases using a 3D U-Net Convolutional Neural Network. Society for Imaging Informatics in Medicine Virtual Meeting 2020.
60. Antinori S, Corbellino M, Meroni L, et al. Aspergillus meningitis: A rare clinical manifestation of central nervous system aspergillosis. Case report and review of 92 cases. J Infect 2013;66(3):218–38. [PubMed: 23178421]
61. Almutairi BM, Nguyen TB, Jansen GH, et al. Invasive Aspergillosis of the Brain: Radiologic-Pathologic Correlation. RadioGraphics 2009;29:375–9. [PubMed: 19325053]
62. Mamelak AN, Obana WG, Flaherty JF, et al. Nocardial Brain Abscess: Treatment Strategies and Factors Influencing Outcome. Neurosurgery 1994;35(4):622–31. [PubMed: 7808604]
63. Ramsey RG, Geremia GK. CNS complications of AIDS: CT and MR findings. AJR Am J Roengenol 1988;151(3):449–54.
64. Kumar GGS, Mahadevan A, Guruprasad AS, et al. Eccentric Target Sign in Cerebral Toxoplasmosis – neuropathological correlate to the imaging feature. J Magn Reson Imaging 2010;31(6):1469–72. [PubMed: 20512900]
65. Fernàndez-Sabé N, Cervera C, Fariñas MC, et al. Risk factors, clinical features, and outcomes of toxoplasmosis in solid-organ transplant recipients: a matched case-control study. Clin Infect Dis 2012;54(3):355–61. [PubMed: 22075795]
66. Ganiem AR, Dian S, Indriati A, et al. Cerebral Toxoplasmosis Mimicking Subacute Meningitis in HIV-Infected Patients; a Cohort Study from Indonesia. PLOS Negl Trop Dis 2013;7(1):e1994. [PubMed: 23326616]
67. Rock RB, Olin M, Baker CA, et al. Central Nervous System Tuberculosis: Pathogenesis and Clinical Aspects. Clin Microbiol Rev 2008;21(2):243–61. [PubMed: 18400795]
68. Chan KH, Cheung RT, Lee R, et al. Cerebral infarcts complicating tuberculous meningitis. Cerebrovasc Dis 2005;19(6):361–5.
69. Raut T, Garg RK, Jain A, et al. Hydrocephalus in tuberculous meningitis: Incidence, its predictive factors and impact on the prognosis. J Infect 2013;66(4):330–7. [PubMed: 23291048]
70. Kim TK, Chang KH, Kim CJ, et al. Intracranial Tuberculoma: Comparison of MR with Pathologic Findings. AJNR Am J Neuroradiol 1995;16:1903–8. [PubMed: 8693993]
71. Rudie JD, Rauschecker AM, Nabavizadeh SA, et al. Neuroimaging of Dilated Perivascular Spaces: From Benign to Pathologic Causes to Mimics. J Neuroimaging 2017;28(2):139–49. [PubMed: 29280227]
72. Liliang P-C, Liang C-L, Chang W-N, et al. Shunt Surgery for Hydrocephalus Complicating Cryptococcal Meningitis in Human Immunodeficiency Virus-Negative Patients. Clin Infect Dis 2003;37(5):673–8. [PubMed: 12942399]
73. Saag MS, Graybill RJ, Larsen RA, et al. Practice Guidelines for the Management of Cryptococcal Disease. Clin Infect Dis 2000;30(4):710–8. [PubMed: 10770733]
74. La Mantia L, Costa A, Eoli M, et al. Racemose neurocysticercosis after chronic meningitis: effect of medical treatment. Clin Neurol Neurosurg 1995;97(1):50–4. [PubMed: 7788974]
75. Zhao J-L, Lerner A, Shu Z, et al. Imaging spectrum of neurocysticercosis. Radiol Infect Dis 2015;1(2):94–102.
76. Kimura-Hayama ET, Higuera JA, Corona-Cedillo R, et al. Neurocysticercosis: Radiologic-Pathologic Correlation. RadioGraphics 2010;30(6):1705–19. [PubMed: 21071384]
77. Verma A, Madhavi, Patwari S, et al. Use of 3D CISS as part of a routine protocol for the evaluation of intracranial granulomas. Indian J Radiol Imaging 2011;21(4):311. [PubMed: 22223948]
78. Cabral DA, Flodmark O, Farrell K, et al. Prospective study of computed tomography in acute bacterial meningitis. J Pediatr 1987;111(2):201–5. [PubMed: 3612390]
79. Kasanmoentalib ES, Brower MC, van der Ende A, et al. Hydrocephalus in adults with community-acquired bacterial meningitis. Neurology 2010;75(10):918–23. [PubMed: 20820003]

80. Sotelo J, Guerrero V, Rubio F. Neurocysticercosis: a new classification based on active and inactive forms: a study of 753 cases. Arch Intern Med 1985;145(3):442–5. [PubMed: 3977513]
81. Ferreira NP, Otta GM, do Amaral LL, et al. Imaging aspects of pyogenic infections of the central nervous system. Top Magn Reson Imaging 2005;16(2):145–54. [PubMed: 16340334]
82. van de Beek D, Campeau NG, Eelco W. The clinical challenge of recognizing infratentorial empyema. Neurology 2007;69(5):477–81. [PubMed: 17664407]
83. Wong AM, Zimmerman RA, Simon EM, et al. Diffusion-weighted MR imaging of subdural empyemas in children. AJNR Am J Neuroradiol 2004;25:1016–21. [PubMed: 15205140]
84. Saremi F, Helmy M, Farzin S, et al. MRI of Cranial Nerve Enhancement. AJR Am J Roentgenol 2005;185(6):1487–97. [PubMed: 16304002]
85. Richardson MP, Reid A, Tarlow MJ, et al. Hearing loss during bacterial meningitis. Arch Dis Child 1997;76(2):134–8. [PubMed: 9068303]
86. Beijen J, Casselman J, Joosten F, et al. Magnetic resonance imaging in patients with meningitis induced hearing loss. Eur Arch Otorhinolaryngol 2009;266(8):1229–36. [PubMed: 19221779]
87. Deliran SS, Brouwer MC, Coutinho JM, et al. Bacterial meningitis complicated by cerebral venous thrombosis. Eur Stroke J 2020;5(4):394–401. [PubMed: 33598558]
88. Liu L-L, Zheng W-H, Tong M-L, et al. Ischemic stroke as a primary symptom of neurosyphilis among HIV-negative emergency patients. J Neurol Sci 2012;317(1–2):35–9. [PubMed: 22482824]
89. Kastenbauer S, Pfister HW. Pneumococcal meningitis in adults: spectrum of complications and prognostic factors in a series of 87 cases. Brain 2003;126:1015–25. [PubMed: 12690042]
90. Mishra AK, Arvind VH, Muliyil D, et al. Cerebrovascular injury in cryptococcal meningitis. Int J Stroke 2018;13(1):57–65. [PubMed: 28421878]
91. Lan SH, Chang WN, Lu CH, et al. Cerebral infarction in chronic meningitis: a comparison of tuberculous meningitis and cryptococcal meningitis. QJM 2001;94(5):247–53. [PubMed: 11353098]
92. Tai M-LS, Viswanathan S, Rahmat K, et al. Cerebral infarction pattern in tuberculous meningitis. Sci Rep 2016;6:38802. [PubMed: 27958312]
93. Wasay M, Khan M, Farooq S, et al. Frequency and Impact of Cerebral Infarctions in Patients With Tuberculous Meningitis. Stroke 2018;49:2288–93. [PubMed: 30355085]
94. Hsieh FY, Chia LG, Shen WC. Locations of cerebral infarctions in tuberculous meningitis. Neuroradiology 1992;34(3):197–9. [PubMed: 1630608]
95. Zhang L, Zhang X, Li H, et al. Acute ischemic stroke in young adults with tuberculous meningitis. BMC Infect Dis 2019;19:362. [PubMed: 31039747]
96. Forgacs P, Geyer CA, Freidberg SR. Characterization of Chemical Meningitis after Neurological Surgery. Clin Infect Dis 2001;32(2):179–85. [PubMed: 11170905]
97. Bier G, Klumpp B, Roder C, et al. Meningeal enhancement depicted by magnetic resonance imaging in tumor patients: neoplastic meningitis or therapy-related enhancement? Neuroradiology 2019;61(7):775–82. [PubMed: 31001647]
98. Morís G, Garcia-Monco JC. The challenge of drug-induced aseptic meningitis revisited. JAMA Intern Med 2014;174(9):1511–2. [PubMed: 25003798]
99. Wilms G, Lammens M, Marchal G, et al. Thickening of dura surrounding meningiomas: MR features. J Comput Assist Tomogr 1989;13(5):763–8. [PubMed: 2778133]
100. Delgado-García G, Ramirez-Bermudez J, Flores-Rivera J, et al. Pachymeningeal Enhancement in Anti-NMDA Receptor Encephalitis. Neurology 2020;94(15):2567.
101. Degnan AJ, Levy LM. Neuroimaging of Rapidly Progressive Dementias, Part 2: Prion, Inflammatory, Neoplastic, and Other Etiologies. AJNR Am J Neuroradiol 2014;35(3):424–31. [PubMed: 23413251]
102. Dumas JL, Valeyre D, Chapelon-Abric C, et al. Central nervous system sarcoidosis: follow-up at MR imaging during steroid therapy. Radiology 2000;214(2):411–20. [PubMed: 10671588]
103. Ganeshan D, Menias CO, Lubner MG, et al. Sarcoidosis from Head to Toe: What the Radiologist Needs to Know. RadioGraphics 2018;38(4):1180–200. [PubMed: 29995619]

104. Pittock SJ, Debruyne J, Krecke KN, et al. Chronic lymphocytic inflammation with pontine perivascular enhancement responsive to steroids (CLIPPERS). Brain 2010;133(9):2626–34. [PubMed: 20639547]

105. Tobin WO, Guo Y, Krecke KN, et al. Diagnostic criteria for chronic lymphocytic inflammation with pontine perivascular enhancement responsive to steroids (CLIPPERS). Brain 2017;140(9):2145–425.

106. Schwartz KM, Erickson BJ, Lucchinetti C. Pattern of T2 hypointensity associated with ring enhancing brain lesions can help to differentiate pathology. Neuroradiology 2006;48:143–9. [PubMed: 16447037]

107. Haldorsen IS, Espeland A, Larsson JL. Central Nervous System Lymphoma: Characteristic Findings on Traditional and Advanced Imaging. Am J Neuroradiol 2011;32(6):984–92. [PubMed: 20616176]

108. Hartmann M, Jansen O, Heiland S, et al. Restricted Diffusion within Ring Enhancement Is Not Pathognomonic for Brain Abscess. Am J Neuroradiol AJNR 2001;22(9):1738–42. [PubMed: 11673170]

Box 1

Conditions with pachymeningeal versus leptomeningeal enhancement

Pachymeningeal	Leptomeningeal
• Intracranial hypotension	• Infectious meningitis
• Infection (syphilis, tuberculosis)	• Inflammatory (sarcoidosis)
• Inflammatory (sarcoidosis)	• Neoplastic meningitis
• Lymphoma/leukemia	
• Neoplastic meningitis	
• Granulomatosis with polyangiitis	

Box 2

Differentiation between normal meningeal vessels versus abnormal leptomeningeal enhancement

Normal Meningeal Vessels/Cortical Veins	Abnormal Leptome-ningeal Enhancement
• Thin, smooth	• Thick, nodular, irregular
• Short, discontinuous, well-demarcated	• Long, continuous, poorly demarcated
• Symmetric	
• Superficial, most prominent parasagitally	• Asymmetric
	• Extends deep to base of sulci
• Short-segment convexity enhancement	• Long-segment (>3cm) or diffuse convexity enhancement
• Isolated fine linear falcine and tentorial enhancement	• If meningeal enhancement present on 3 contiguous axial spin echo MR images
• No enhancement of cisterns, ventricular walls	

Box 3

Imaging features of bacterial meningitis

- Most common finding is a normal scan
- Effaced CSF spaces
- Poorly visualized basilar cisterns
- Generalized cerebral edema
- Diffuse leptomeningeal enhancement
- Communicating hydrocephalus
- Subdural effusion (in children)/empyema
- Hyperintense sulcal signal abnormalities on FLAIR
- Subtle subarachnoid/ventricular high signal pus on DWI
- Sometimes associated with cranial nerve enhancement

Box 4

Common clinical findings in meningitis

Infants	Adults
• Fever	• Fever
• Irritability	• Headache
• Constipation	• Nuchal rigidity
• Vomiting	• Brudzinski/Kernig sign
• Kernig sign	
• Seizures	• Altered mental status
• Altered sensorium	• Photophobia
• Bulging fontanelle	• Rash
	Older Adults
• Anorexia	• Fever
• Failure to thrive	• Lethargy

Box 5

Differential diagnosis of sulcal hyperintensity on fluid attenuated inversion recovery MR imaging

- Meningitis
- Subarachnoid hemorrhage
- Leptomeningeal carcinomatosis
- Slow flow through pial collaterals in acute stroke
- Moyamoya disease
- Increased blood pool/CSF ratio
- Supplemental oxygen
- Artifact: Pulsation, magnetic susceptibility, motion

Box 6

Common causes of acute meningitis by age

Newborn <4 weeks	Adults
• Group B streptococci	• *S pneumoniae* • *N meningitidis*
• *Escherichia coli*	• Enteroviruses
• *Listeria monocytogenes*	• Herpes simplex
Children	Older Adults
• *H influenzae type b*	• *S pneumoniae*
• *N meningitidis*	• *N meningitidis*
• *S pneumoniae*	• *L monocytogenes*
• *Enteroviruses*	• Aerobic Gram-negative bacilli

Box 7

Causes of eosinophilic meningitis

- *Angiostrongylus cantonensis*
- *Gnathostoma spinigerum*
- *Taenia solium*
- *Trichinella spiralis*
- *Toxocara canis*
- *Loa loa*
- *Mansonella perstans*
- *Coccidioides immitis*
- Intrathecal injection of foreign proteins
- CNS insertion of rubber tubing

Box 8

Clinical features suspicious of developing abscess

- Relentless headache
- Fever
- Worsening neurologic deficits
- Altered mental status
- Nausea and vomiting
- New seizures
- Developing papilledema

Box 9

MR spectroscopy findings of pyogenic abscess

Decreased or not Elevated neuron metabolites	Increased inflammation
	• Lactate (1.33 ppm)
• *N*-acetyl-aspartate (2.0 ppm)	• Lipids (0.9–1.3 ppm)
• Creatine (3.0 ppm)	Elevated and specific to infection
• Choline (3.2 ppm)	• Valine, leucine, isoleucine (0.9 ppm)
	• Succinate (2.4 ppm)
	• Acetate (1.9 ppm)

Box 10

Common causes of brain abscess

Immunocompetent	Immunocompromised
• *S aureus*	• *Aspergillus*
• *E coli*	• *Cryptococcus*
• *Enterobacter*	• *Toxoplasma*
• *Actinomyces*	• *Nocardia*
• *Bacteroides*	• *Candida*
• *Prevotella*	• *Mucor, Rhizopus*

Box 11

Causes of drug-induced meningitis

- NSAIDs: ibuprofen, celecoxib, naproxen
- Antibiotics: trimethoprim/sulfamethoxazole, amoxicillin, metronidazole, ciprofloxacin
- Immunomodulatory agents: sulfasalazine, azathioprine, capecitabine, methotrexate
- Immunotherapies: IV-IG, cetuximab, adalimu-mab, infliximab, nivolumab, pembrolizumab, ipilimumab, muromonab
- Antiepileptics: lamotrigine, carbamazepine

Box 12

Differential diagnosis of ring and peripheral enhancement

- Metastasis
- Abscess
- Glioma, Lymphoma
- Infarct
- Contusion
- Demyelination
- Resolving hematoma
- Radiation necrosis

KEY POINTS

- Neuroimaging can confirm clinical suspicion for infection, rule out mimics, assist/replace/complement lumbar puncture and assess for complications including abscess, ventriculitis, extra-axial collections, hydrocephalus, herniation, cranial neuropathy, thrombosis, infarct and vasculitis.
- In acute bacterial meningitis, meningeal enhancement is often located along the cerebral convexity. Chronic and atypical forms of meningitis are usually prominent in the basal cisterns.
- Cerebritis can progress to abscess, which is commonly noted for ring enhancement and centrally restricted diffusion.
- Meningitis, cerebritis, and abscess are included in a wide variety of differential diagnoses related to altered mental status and headaches, so it is imperative to integrate radiographic and clinical information.
- Advanced neuroimaging techniques such as MRS, PET, and artificial intelligence may improve diagnosis of intracranial infections.

CLINICS CARE POINTS

- Meningitis appears as meningeal enhancement along the cerebral convexities and basal cisterns. Complications include abscess, ventriculitis, extra-axial collections, hydrocephalus, herniation, cranial neuropathy, thrombosis, infarction and vasculitis.
- Cerebritis leads to abscess, which is supported by ring enhancement, central diffusion restriction on DWI and often elevated amino acids, succinate and/or acetate on MRS.
- The differential diagnosis for meningeal enhancement and ring enhancement patterns is broad and should be guided by additional imaging and clinical factors.

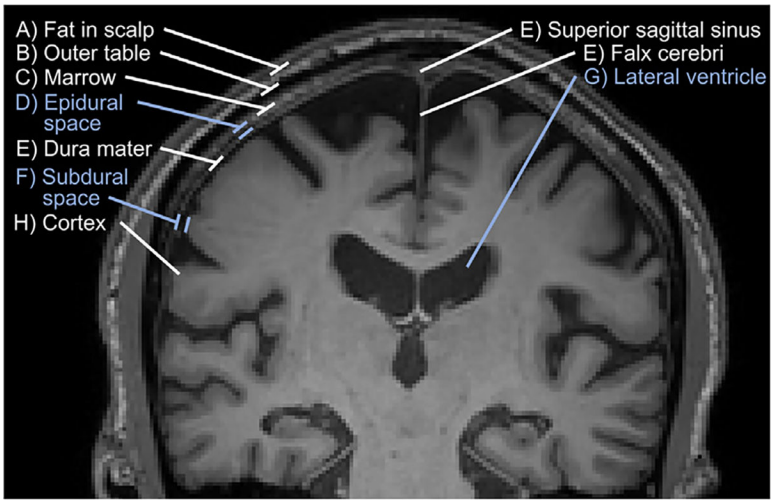

Fig. 1.

Coronal T1-weighted MR imaging shows the meningeal layers and spaces in an older adult. Fat in scalp (A) and outer table (B). Bone marrow (C). Epidural space (D). Dura mater (E), including the superior sagittal sinus and falx cerebri. Subdural space (F). Arachnoid mater is not visualized on imaging. Subarachnoid space including the lateral ventricles (G). Cerebral cortex (H).

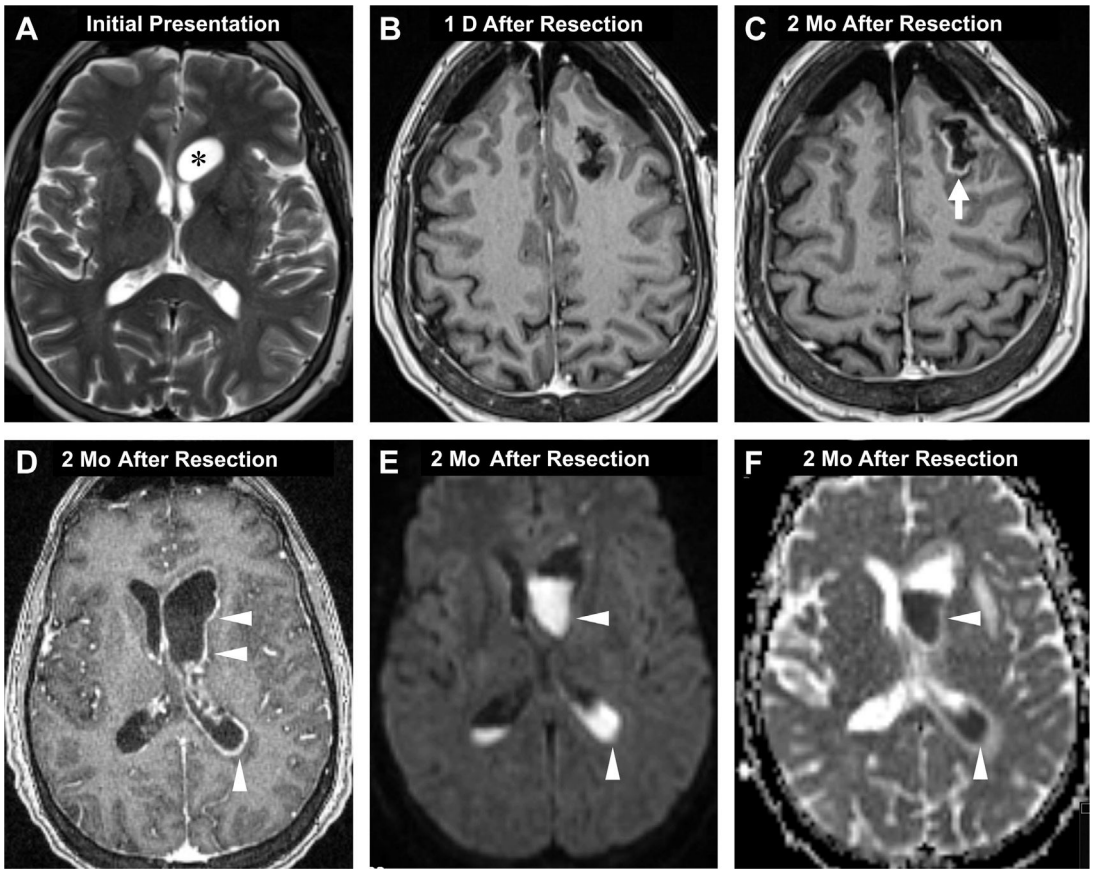

Fig. 2.

Postsurgical CNS infection. T2-weighted MR imaging shows a low-grade cystic glioma abutting the left frontal horn (*asterisk, A*) before craniotomy/resection (*A*). Postoperative day one, axial T1 postcontrast image shows bilateral pneumocephalus with no enhancement around the resection cavity (*B*). Two months later, the patient presented with a seizure. T1 postcontrast MR imaging now depicts peripheral enhancement around the cavity (*arrow, C*) meningitis and ependymitis (*arrowheads*, D) and diffusion restricting, gravity-dependent pus-fluid meniscus levels (*arrowheads*, *E, F*) in the ventricles on DWI (*E*) and ADC (*F*), suggestive of meningitis, ventriculitis, and abscess.

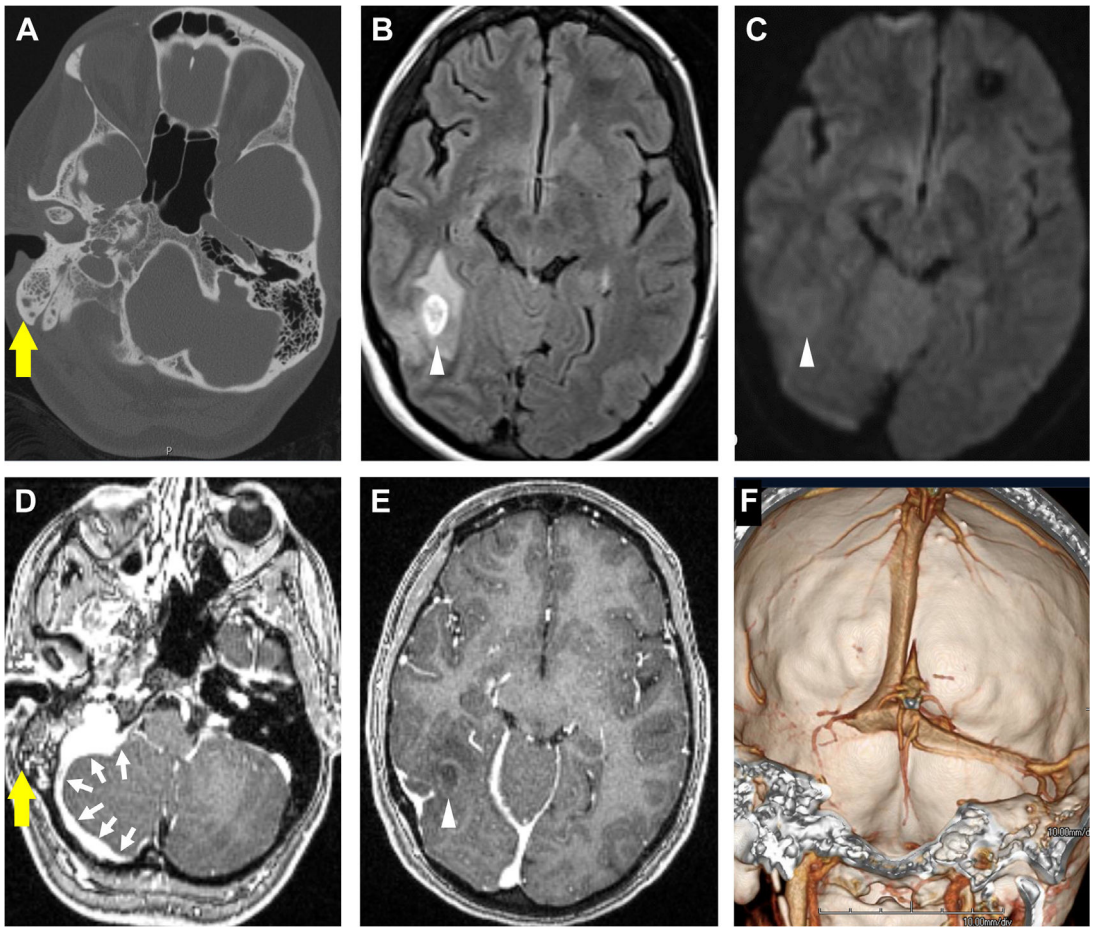

Fig. 3.

Mastoiditis with intracranial complications of CNS infection in a patient presenting with headaches. Opacification of right mastoid air cells on CT (*yellow arrow, A*) is consistent with mastoiditis. Evidence of intracranial complications includes an FLAIR hyperintense lesion (*arrowhead, B*) that does not diffusion restrict on DWI (*arrowhead, C*). On T1 postcontrast (D), there is enhancement in the opacified mastoid air cells (*yellow arrow, D*) with adjacent pachymeningitis (*multiple white arrows, D*). Note the faintly ring-enhancing lesion in the posterior temporal lobe (*arrowhead, E*) on T1 postcontrast, indicative of cerebritis. Venous sinus thrombosis and thrombophlebitis of the right transverse sinus is seen on 3D shaded surface display volume rendering of CT venogram (*F*).

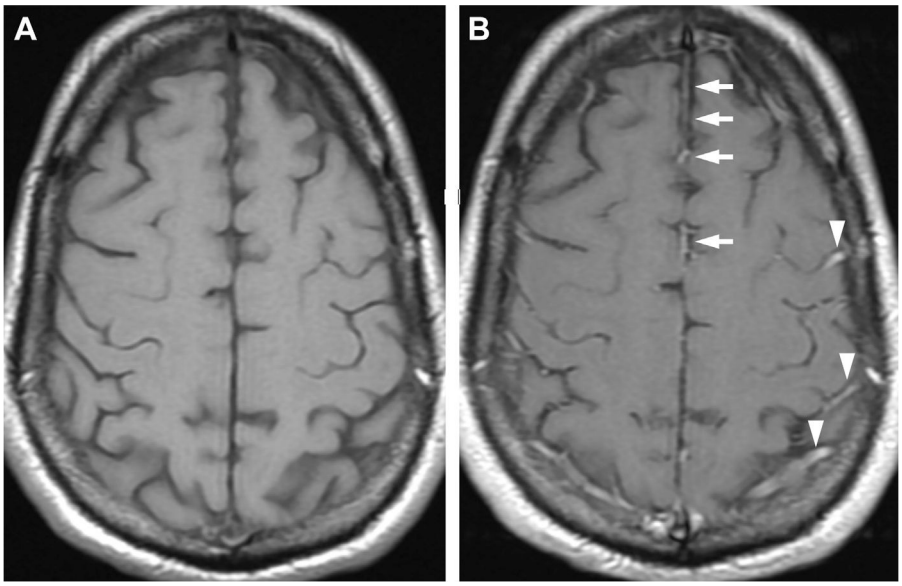

Fig. 4.

Patterns of normal enhancement in precontrast (*A*) and postcontrast MR imaging (*B*) along the anterior falx (arrows) and normal meningeal vessels/cortical veins running in the cerebral sulci (*arrowheads*).

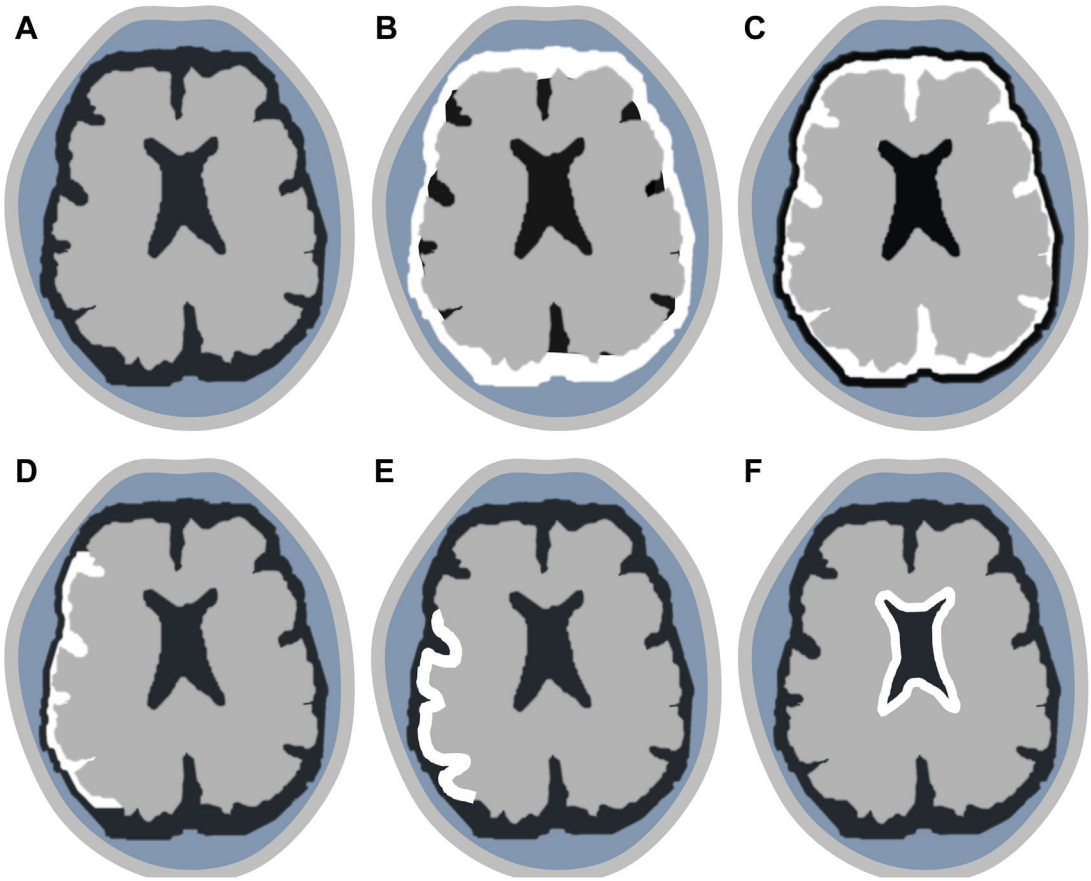

Fig. 5.

Patterns of meningeal contrast enhancement (*white outlines*). Normal meninges (*A*). Diffuse pachymeningeal (*B*). Diffuse leptomeningeal (*C*) and localized leptomeningeal (*D*). Gyriform cortical (*E*). Ependymal (*F*).

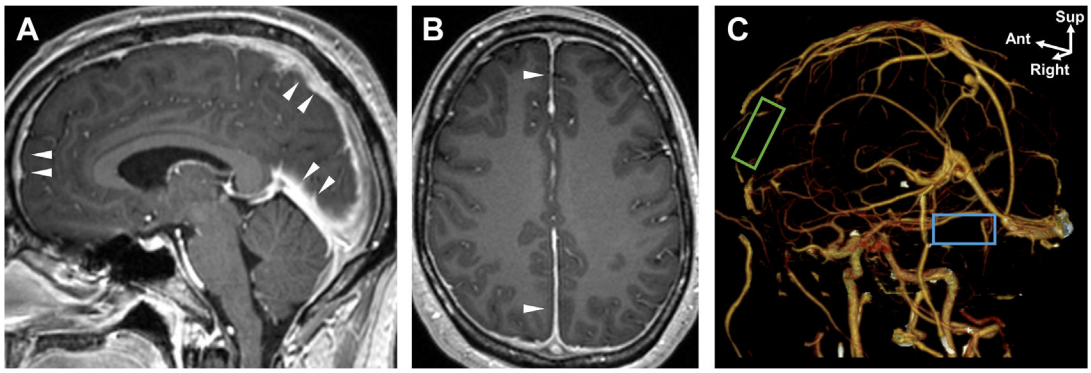

Fig. 6.

Pachymeningeal enhancement in noninfectious granulomatosis with polyangiitis. (*arrowheads, A, B*). Diffuse pachymeningeal enhancement on MR imaging was complicated with chronic dural venous sinus thrombosis of the superior sagittal sinus (*empty green box*, C) and right transverse sinus (*empty blue box, C*) on an oblique view of CT venogram 3D reconstructions (*C*).

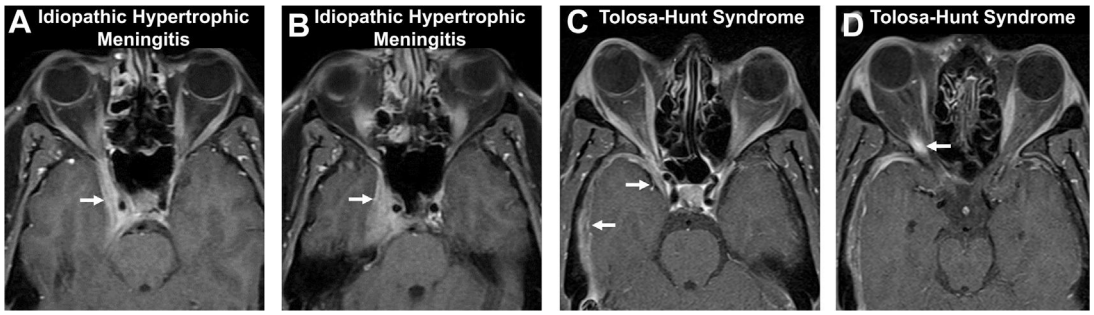

Fig. 7.

Pachymeningeal enhancement in idiopathic hypertrophic meningitis (*A, B*) and Tolosa-Hunt syndrome (*C, D*) on axial T1 postcontrast images. A patient with painless vision loss shows pachymeningeal enhancement (arrows, *A, B*) of the right cavernous sinus, consistent with idiopathic hypertrophic meningitis. Another patient with painful ophthalmoplegia, sudden diplopia, and right proptosis (*C*) demonstrates pachymeningeal enhancement along the right middle cranial fossa and cavernous sinus (*arrows, C*) and orbital apex (*arrow*, *D*) with orbital edema and fat stranding (not shown), consistent with Tolosa-Hunt syndrome.

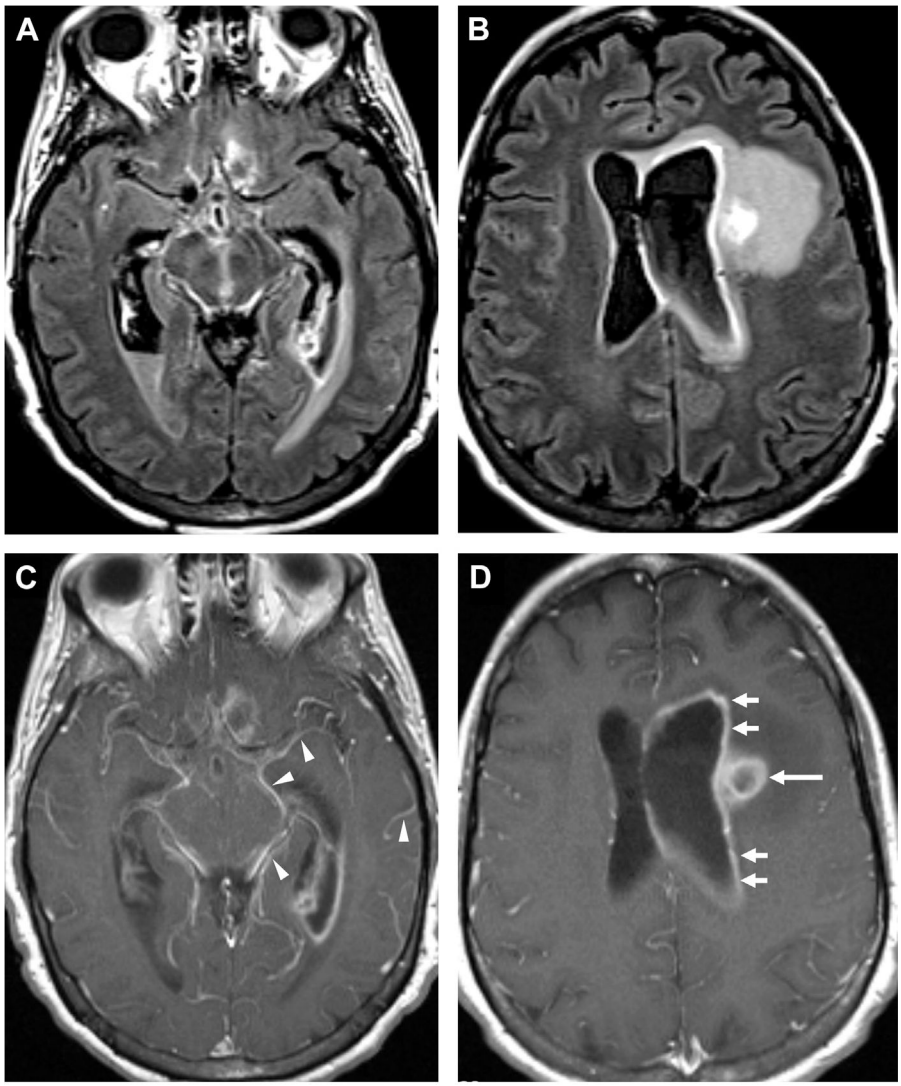

Fig. 8.

Leptomeningeal and ependymal enhancement in bacterial meningitis. FLAIR (*A, B*) and T1 postcontrast MR imaging (*C, D*) in a patient status-post craniotomy shows leptomeningeal enhancement around the midbrain, adjacent sulci and cisterns (*arrowheads*, *C*) and ependymal surface of the left lateral ventricle (*arrows*, *D*). Note the ring-enhancing lesion (*long arrow*, *D*) consistent with abscess.

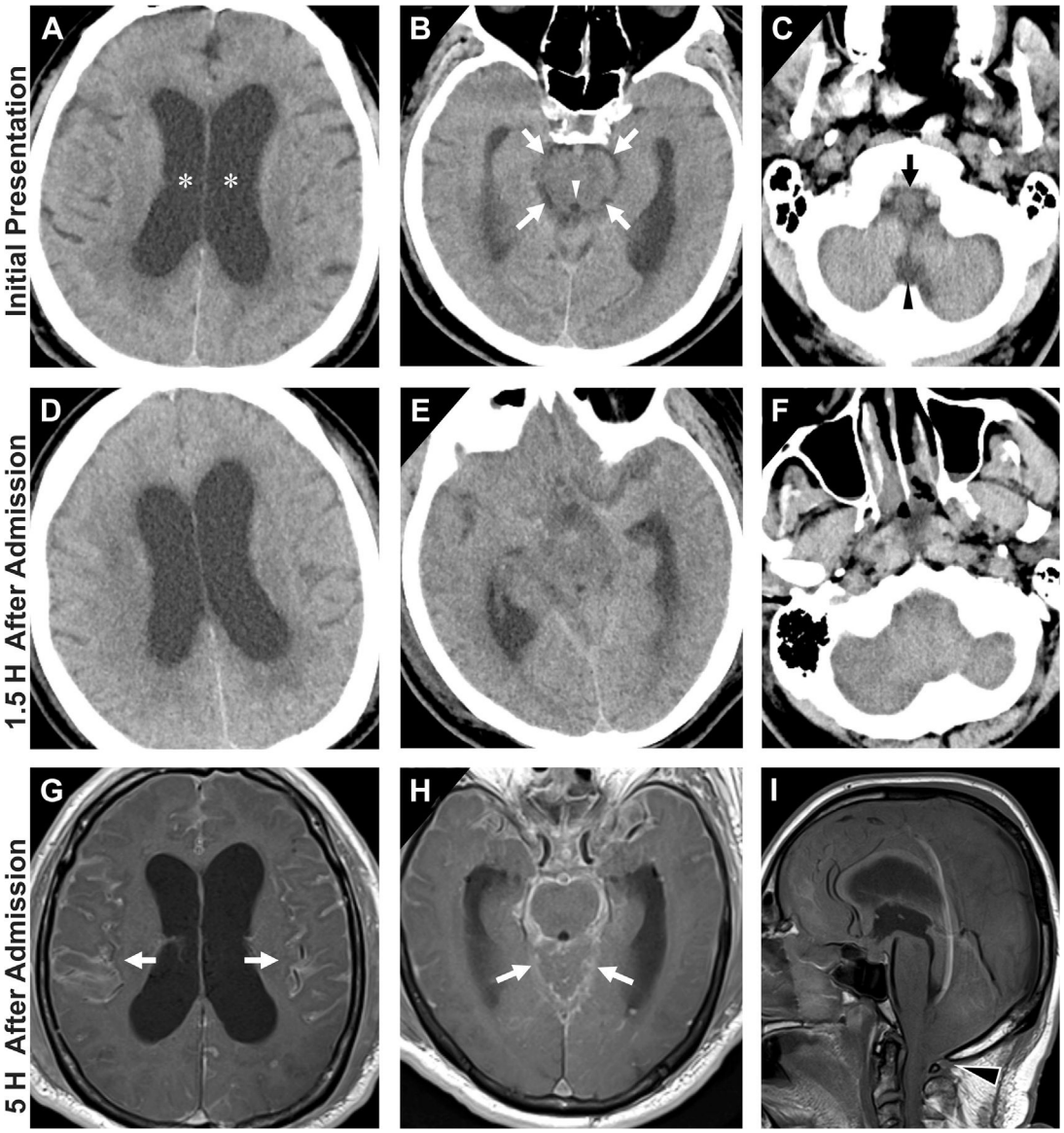

Fig. 9.

Progressive effacement of the basal cisterns on CT in an older adult with altered mental status at initial presentation (*A, B, C*) with interval changes on follow-up CT (*D, E, F*) and MR imaging (*G, H, I*). On admission, there is prominence of bilateral lateral ventricles (*asterisks, A*) with narrower yet still visible CSF-density in perimesencephalic cisterns (*white arrows, B*), cerebral aqueduct (*white arrowhead, B*), perimedullary cistern (*black arrow, C*) and cisterna magna (*black arrowhead, C*). Within 1.5 hours of admission, patient deteriorated clinically and a follow-up head CT demonstrated similar appearance of lateral ventricles (*D*) but interval marked effacement of perimesencephalic and perimedullary cisterns (*E, F*). By 5 hours after admission, T1 postcontrast MR imaging noted diffuse enhancement of cerebral sulci (*arrows, G*), around the brainstem and posterior fossa (*arrows, H*). Notice significant worsening mass effect and cerebral swelling with tonsillar herniation on sagittal T1-weighted MR imaging (*black arrowhead, I*). Mental status decline

corresponded to progressive cerebral swelling and herniations and the patient subsequently passed away.

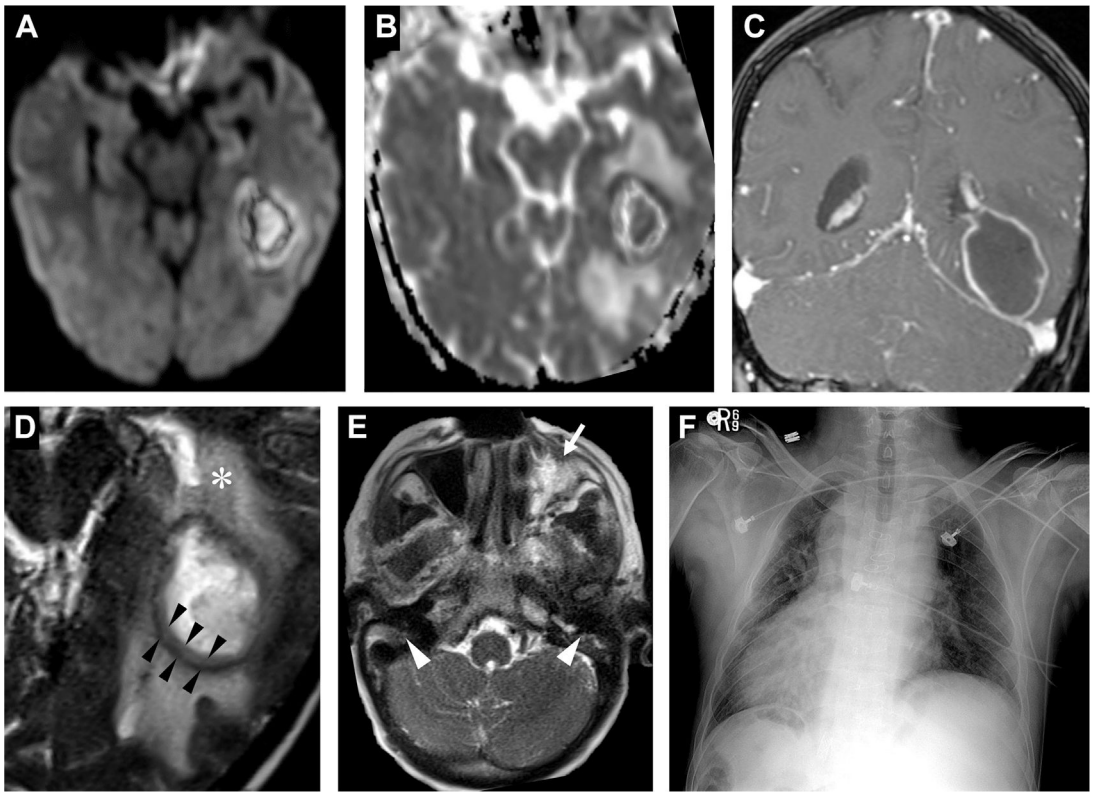

Fig. 10.

Abscess in a patient with primary ciliary dyskinesia (Kartagener syndrome). The left temporal lesion shows restricted diffusion on DWI (*A*) and ADC (*B*) and peripheral-enhancement on T1 postcontrast (*C*). A close-up of the T2-weighted MR imaging portrays a capsule with 2 T2 hypointense layers suggestive of the "dual rim sign" (*black arrowheads, D*) and vasogenic edema (*asterisk, D*). On axial T2 image, notice the left maxillary sinus inflammatory disease (*white arrow, E*) and underdeveloped bilateral mastoid air cells (*white arrowheads, E*) from ciliary dysfunction. Chest X-ray (*F*) portrays situs inversus totalis, typical of primary ciliary dyskinesia.

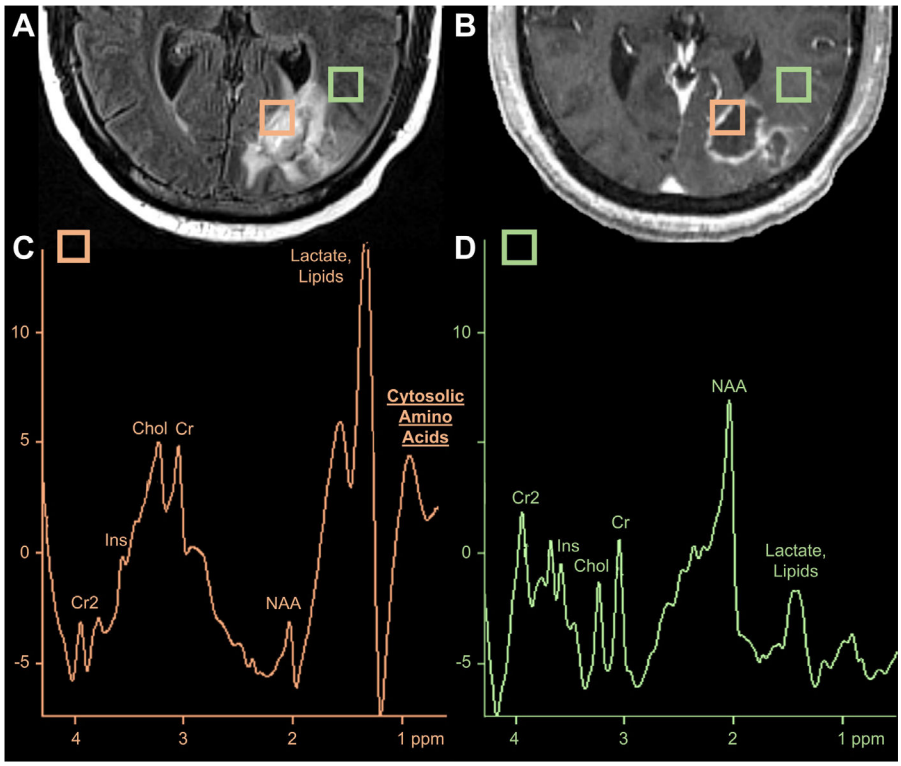

Fig. 11.

Fungal abscess on MR imaging and MRS. An FLAIR hyperintense (*A*), peripherally enhancing abscess (*B*) in the left occipital lobe. The orange square denotes placement of voxel including the abscess cavity while the green square depicts an unaffected region adjacent to the edematous abscess. Comparison of MRS peaks from the abscess cavity (C) and perilesional edematous region (*D*) reveals elevated cytosolic amino acids (0.9 ppm) and lactate/lipids (1.3 ppm) with decreased *N*-acetyl-aspartate (NAA, 2.0 ppm), choline (Cho, 3.0 ppm) and creatine (Cr, 3.2 ppm), consistent with an abscess.

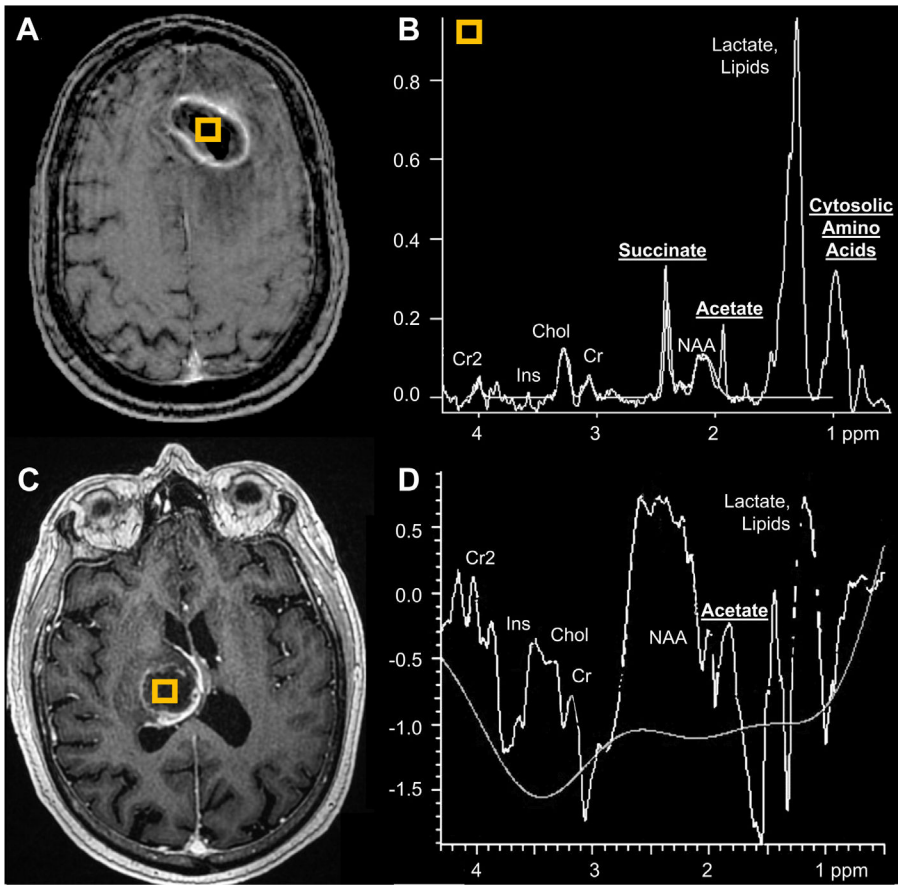

Fig. 12.

Two patients with bacterial abscesses displaying acetate peaks on MRS. T1 postcontrast shows a left frontal abscess with (voxel, *A*). MRS (*B*) depicts elevated succinate (2.4 ppm), acetate (1.9 ppm), amino acids (0.9 ppm), and lactate/lipid (1.3 ppm) peaks and low NAA (2.0 ppm). In a second patient, T1 postcontrast MR imaging depicts a right thalamic abscess (voxel, *C*) with acetate peak and low NAA on MRS (*D*).

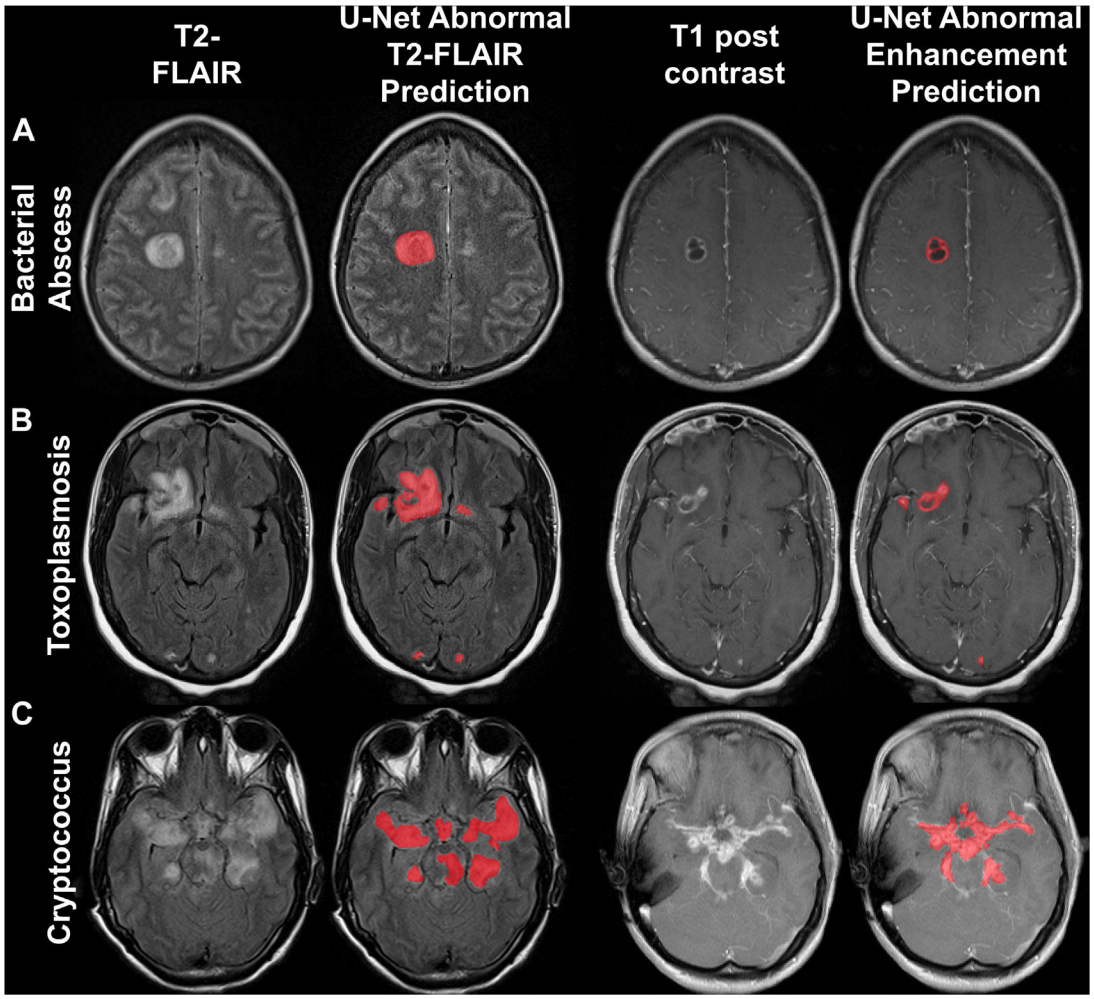

Fig. 13.

Predictions of T2 FLAIR (*left*) and T1 postcontrast (*right*) MR imaging lesions of CNS infections with a deep learning U-net model. Abscess (*A*), toxoplasmosis (*B*), cryptococcosis (*C*).

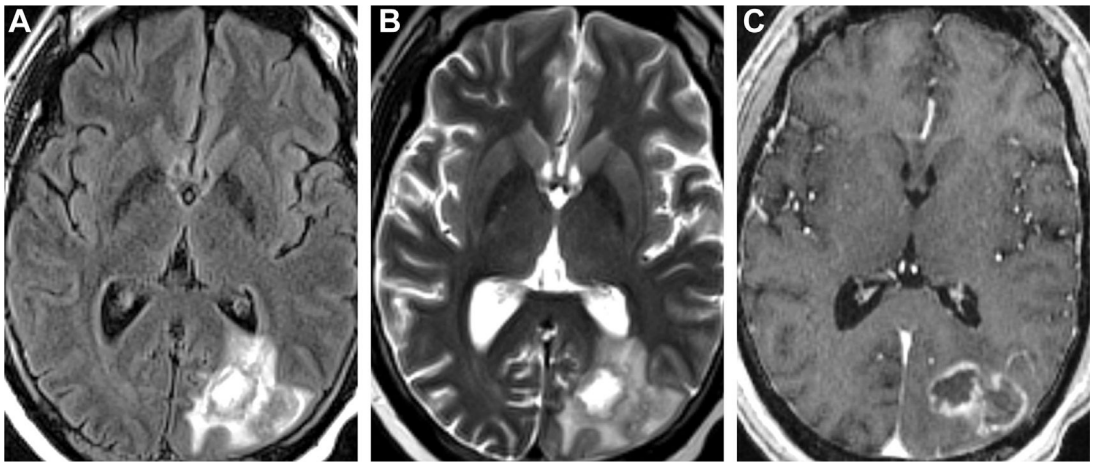

Fig. 14.

Aspergillosis in a patient with graft-versus-host disease presenting with right inferior quadrantanopia. A bilobed abscess in the left occipital region seems FLAIR hyperintense (*A*) with T2 hypointense capsule (*B*) and peripheral enhancement (*C*) and perilesional edema (*A, B*).

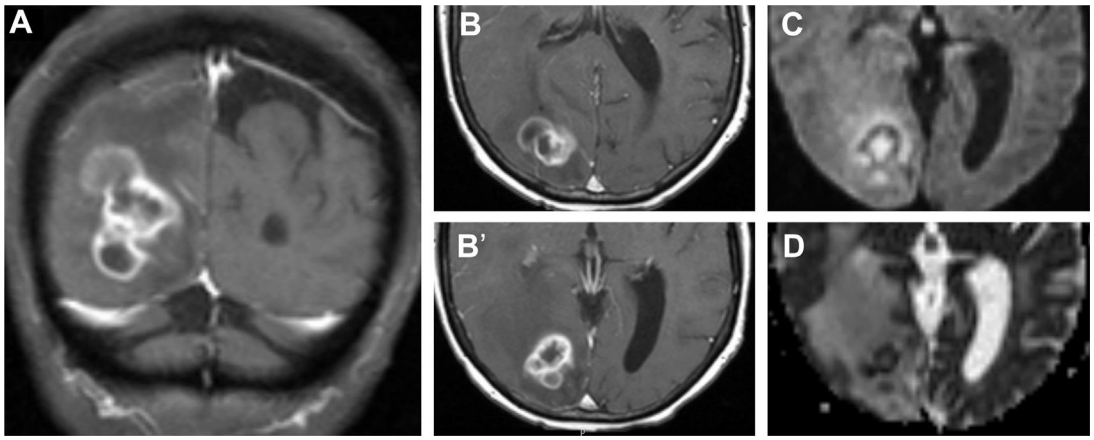

Fig. 15.

Nocardiosis in a patient with leukemia complicated by graft-versus-host disease. T1 postcontrast MR imaging in coronal (*A*) and axial (*B, B'*) planes visualize a multiloculated ring enhancing nocardial abscess in the right parietooccipital region with restricted diffusion on DWI (*C*) and ADC (*D*).

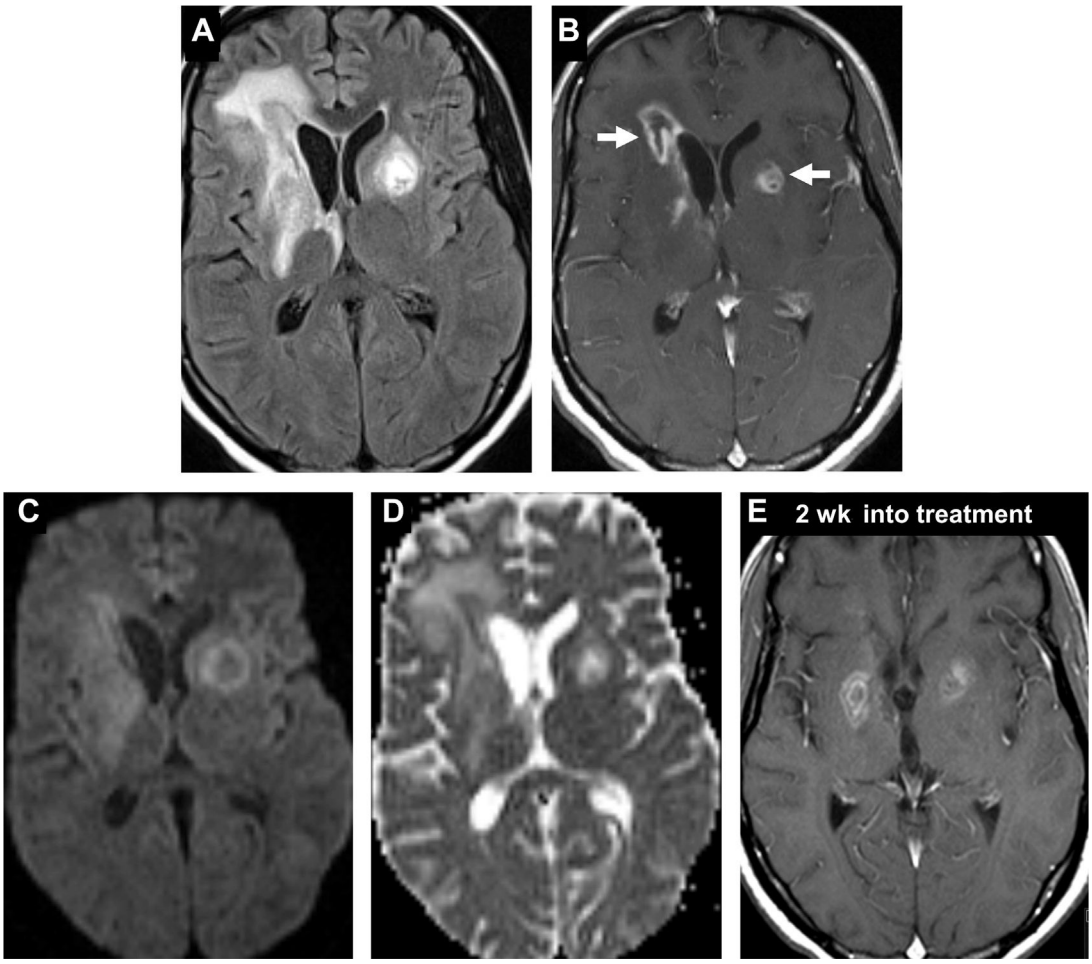

Fig. 16.

Toxoplasmosis in an HIV-positive patient. Ill-defined heterogenous lesions on FLAIR with surrounding vasogenic edema (*A*) and peripheral enhancement (*B*) are evident in the bilateral basal ganglia (*arrows*, *B*). Unlike typical abscess, there is facilitated diffusion on DWI (*C*) and ADC (*D*). Two weeks after initiating antitoxoplasma treatment (*E*), there is interval reduction in enhancement of the lesions, with decreased vasogenic edema (not shown). Note, “eccentric target sign” (*arrow, B*).

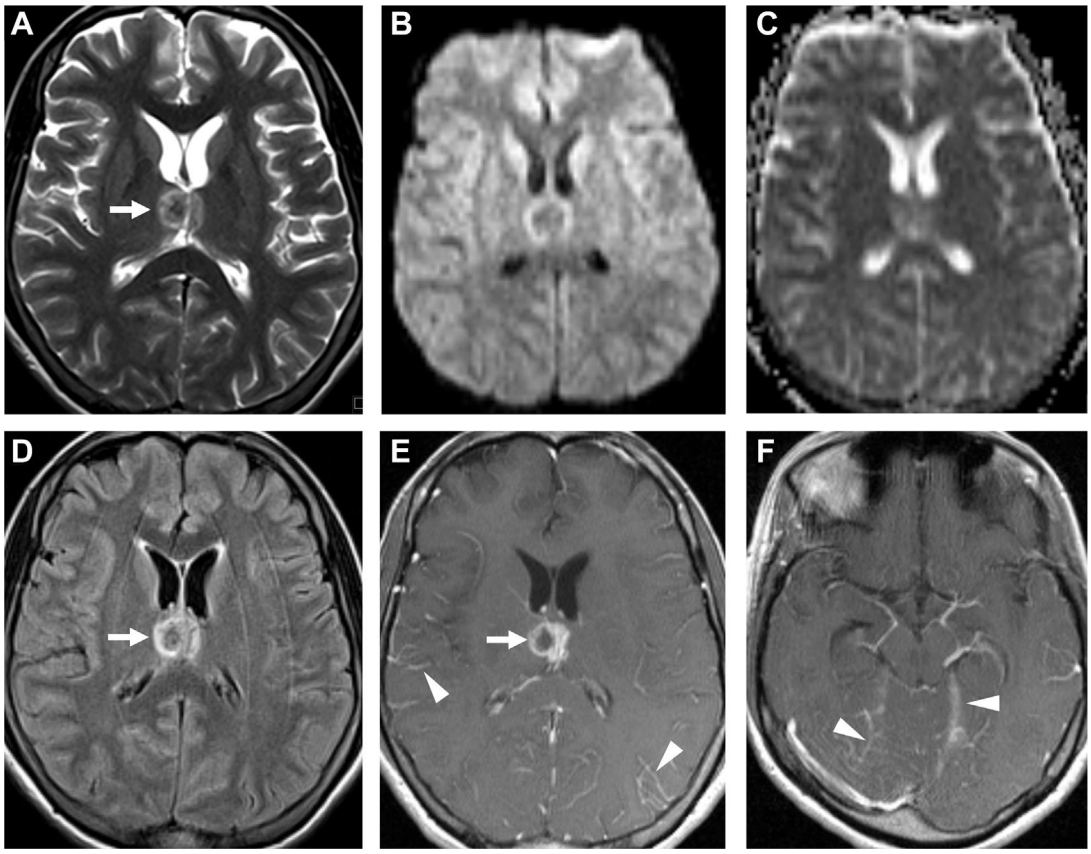

Fig. 17.

Tuberculoma with meningitis. A thalamic lesion with central T2 hypointensity (*arrow, A*), characteristic for tuberculoma, with no restricted diffusion on DWI (*B*) and ADC (*C*) but with FLAIR hyperintensity (*arrow, D*). On T1 postcontrast, there is ring enhancement (*arrow, E*) and associated meningitis (*arrowheads, E, F*).

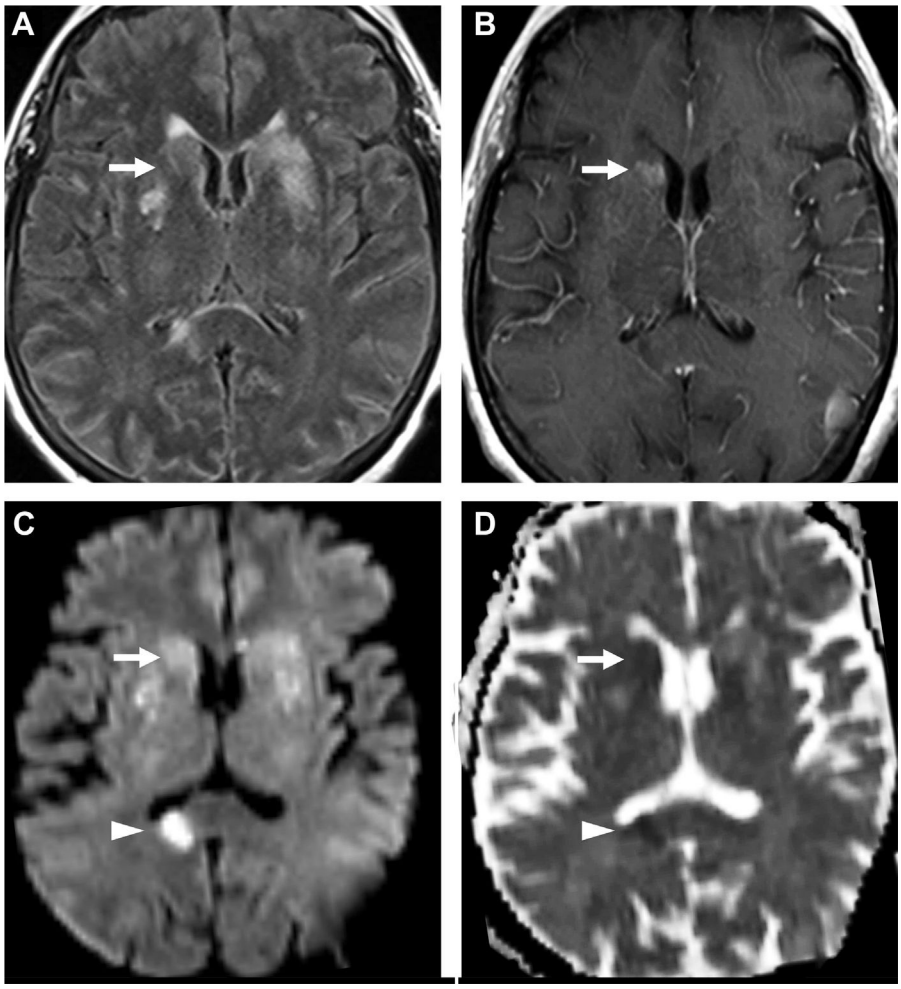

Fig. 18.

Cryptococcosis with meningitis and acute infarction. Multifocal FLAIR hyperintense cryptococcomas are seen in the basal ganglia (*arrows*, *A*) and corpus callosum with enhancement in the right caudate nucleus (*arrow, B*) and bilateral cerebral sulci (B). Diffusion restriction in a right splenium of corpus callosum suggesting acute infarct (arrowhead, C, D) and faint diffusion abnormality in the basal ganglia (arrow, *C, D*) on DWI (*C*) and ADC (*D*).

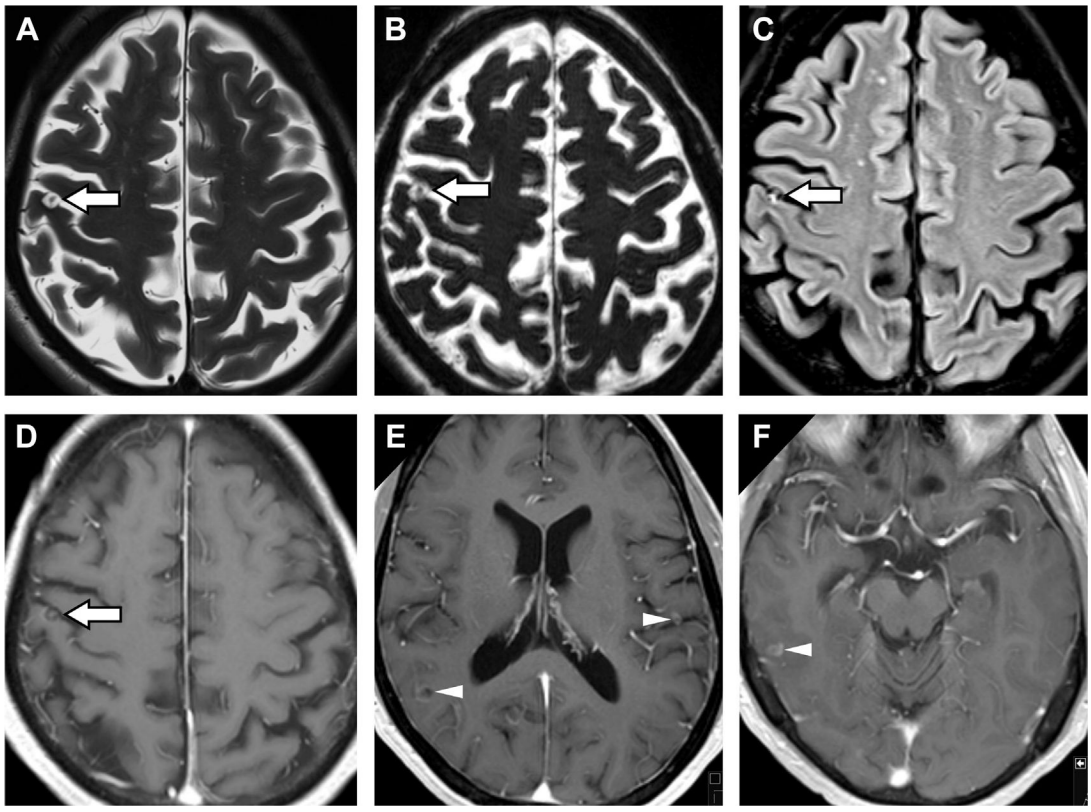

Fig. 19.

Neurocysticercosis in a patient with seizures. A right posterior frontal cystic lesion seen along the pial surface seems with a T2 hypointense inner “dot in a hole” sign (*arrows, A, B*) on T2-weighted (*A*) and T2-weighted thin-section 3D constructive interference in steady state (*B*) images, pathognomonic for the scolex in neurocysticercosis. This cyst is FLAIR hyperintense (*arrow, C*) with central and ring enhancement (*arrow, D*). T1 postcontrast MR imaging reveals leptomeningeal enhancement (*D, E, F*) and additional ring enhancing cysts in the right parietal lobe (*arrowhead, E*), left frontal operculum (*arrowhead, E*) and right lateral temporal lobe (*arrowhead, F*).

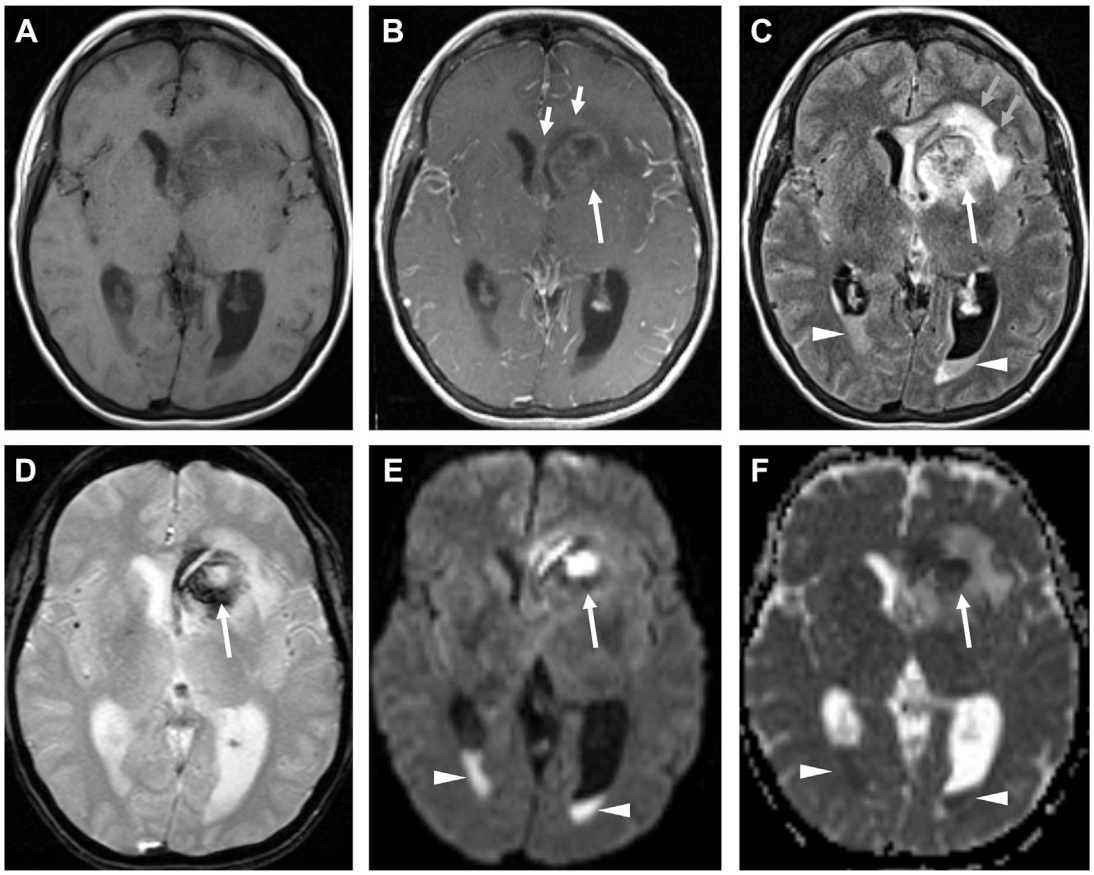

Fig. 20.

Ventriculitis associated with ruptured abscess (*long arrow*, B–D). Axial T1-weighted precontrast (*A*) and postcontrast MR images (*B*) demonstrate a peripherally enhancing left caudate abscess (*long arrow, B*) with subtle linear enhancement of the ependyma of the left frontal horn and midline septum (*short arrows, B*) and diffuse leptomeningeal enhancement. The left caudate abscess is surrounded by vasogenic edema (*short blue arrows, C*), and has ruptured in the ventricles, susceptibility from blood products on GRE (long arrow, D) and restricted diffusion (*long arrows, E, F*) on DWI (*E*) and ADC (*F*). Notice a lack of susceptibility of the dependent debris in the occipital horns on GRE, with corresponding FLAIR hyperintensity (*arrowheads, C*) and restricted diffusion (*arrowheads, E, F*), consistent with layering pus.

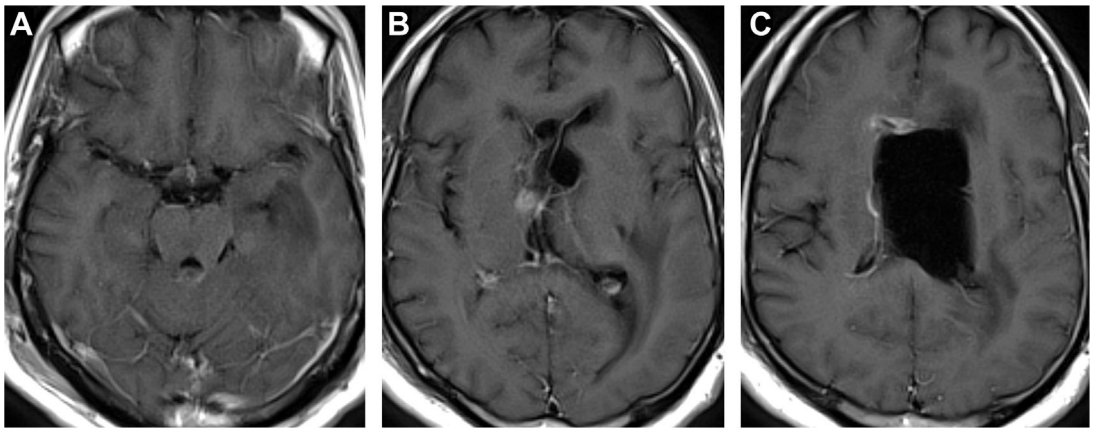

Fig. 21.

Cryptococcosis and hydrocephalus. T1 postcontrast MR imaging visualizes subtle perimesencephalic and bilateral posterior leptomeningeal enhancement (*A*). Enhancement along an obstructed foramen of Monro (*B*). Ependymal enhancement with enlarged left lateral ventricle (*C*). The right lateral ventricle is reduced in volume due to left ventricle compression and drainage by a ventriculostomy catheter.

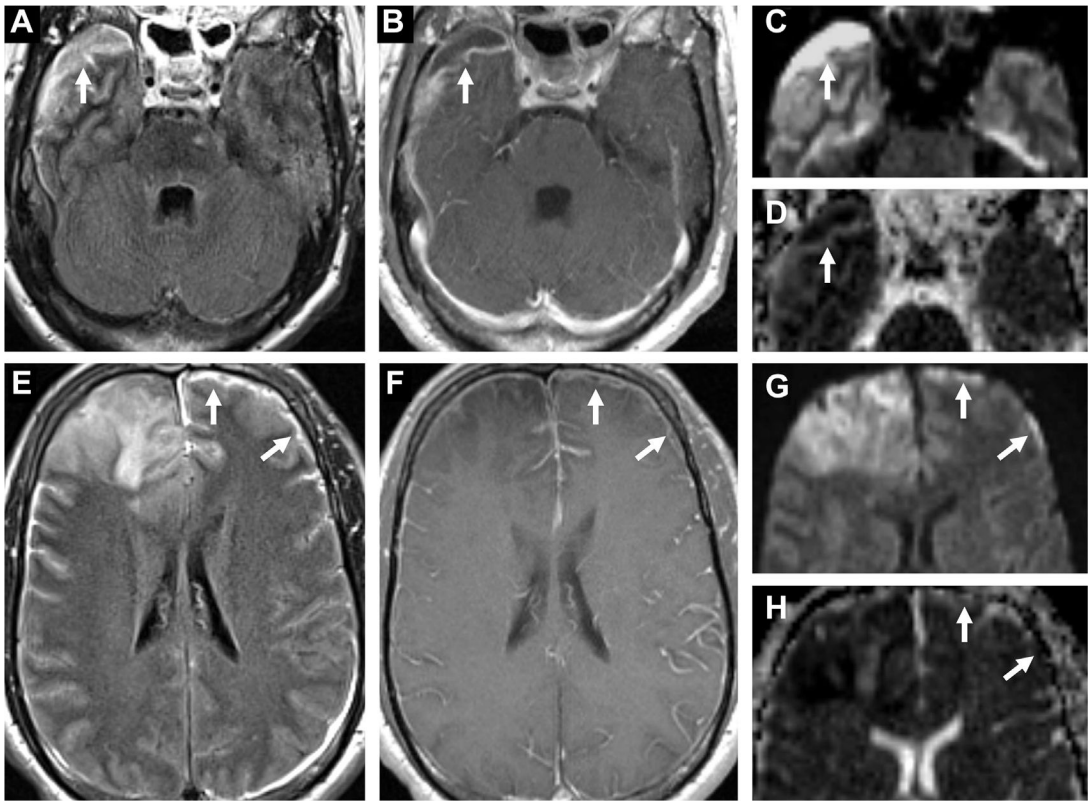

Fig. 22.

Subdural empyema in a patient with bacterial meningitis and cerebritis. A crescentic subdural collection in the right middle cranial fossa (*arrows*) is FLAIR hyperintense (*A*) with enhancement (*B*) and restricted diffusion on DWI (*C*) and ADC (*D*). In the left anterior convexity (*arrows*), a thin FLAIR hyperintense collection (*E*) with leptomeningeal enhancement (*F*) shows diffusion restriction on DWI (G) and ADC (*H*). Note also diffuse leptomeningitis (*F*) and frontal cerebritis, right worse than left (*E–H*).

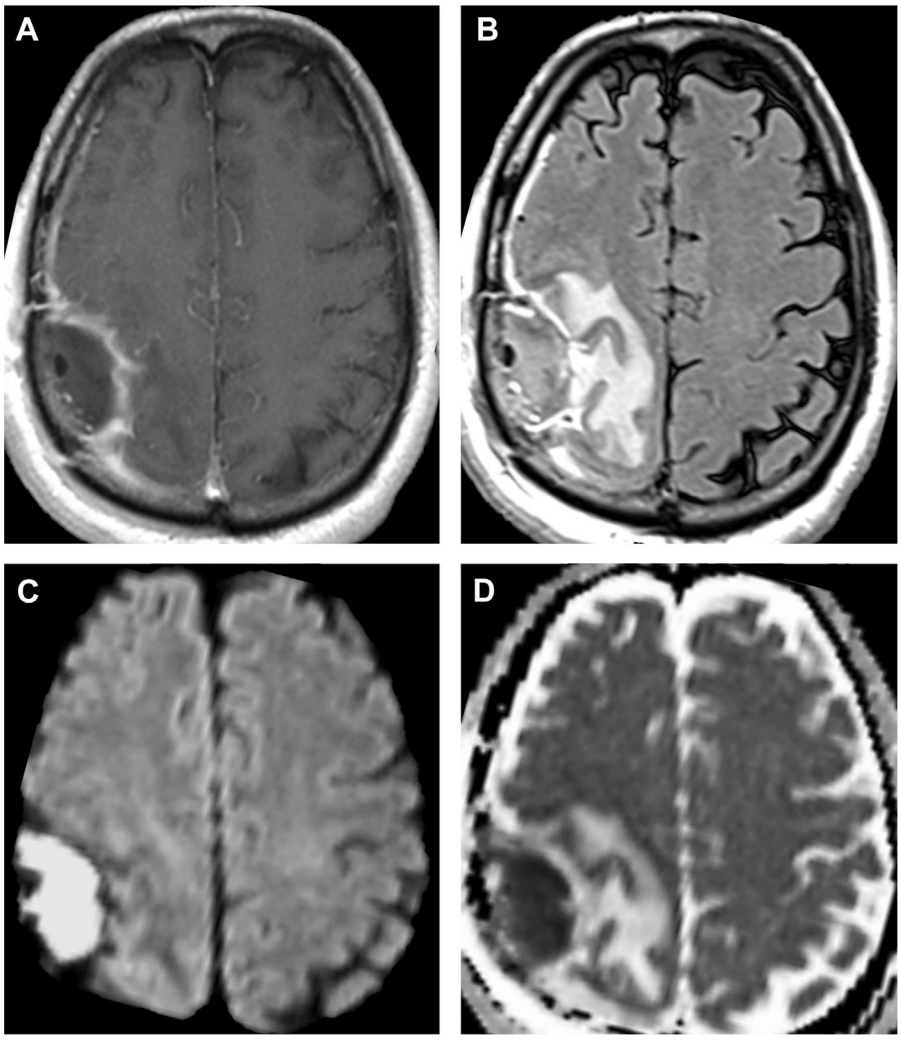

Fig. 23.

Epidural empyema in bacterial meningitis. This seems as a biconvex collection with thick peripheral enhancement (*A*) subjacent the craniotomy site with FLAIR hyperintensity (*B*) and diffusion restriction on DWI (*C*) and ADC (*D*) maps.

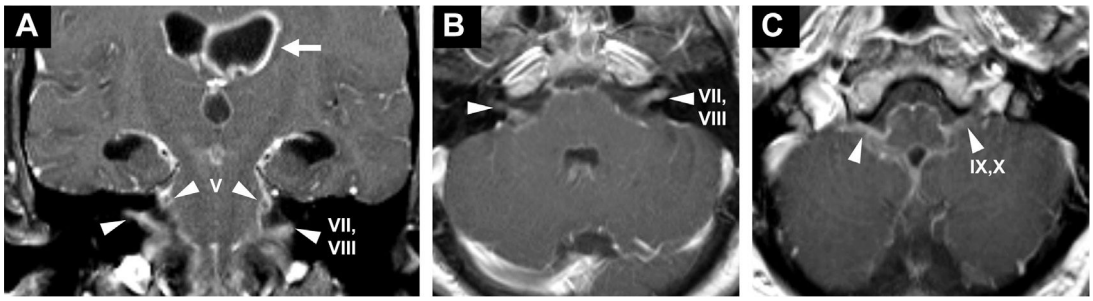

Fig. 24.

Cranial neuropathy in a patient with bacterial leptomeningitis presenting with dilated, fixed pupils lacking several cranial nerve (CN) reflexes. T1 postcontrast images demonstrate enhancement of bilateral trigeminal nerves (CN V, *arrowheads*, *A*), facial/vestibulocochlear nerves (CN VII, VIII, *arrowheads*, *A, B*) and glossopharyngeal/vagus nerves (CN IX, X, *arrowheads*, *C*). Thick ependymal enhancement is noted (*arrow*, *A*).

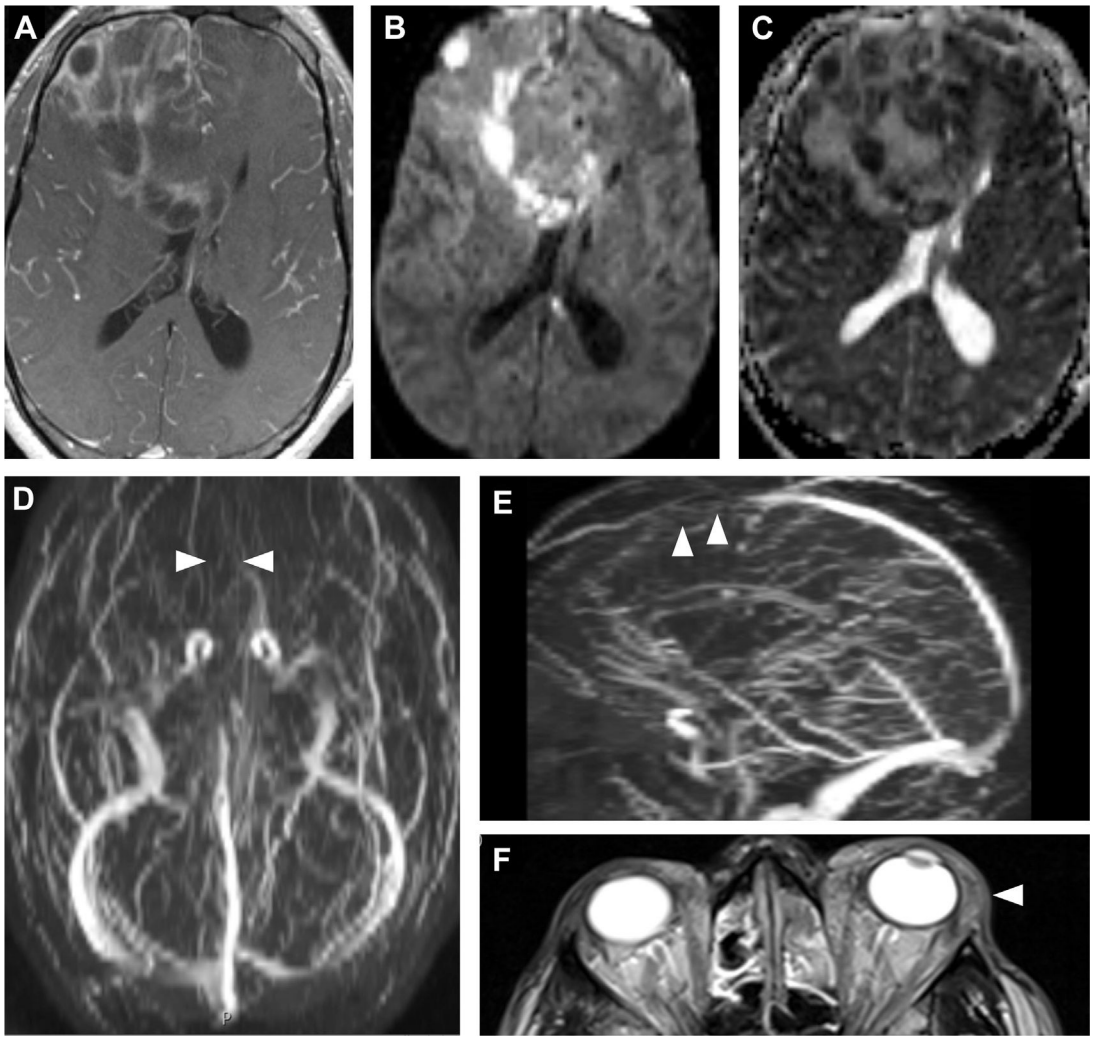

Fig. 25.

Venous sinus thrombosis in an immunocompromised patient with MRSA bacteremia, sinusitis, and orbital cellulitis. Axial T1 postcontrast MR imaging (*A*) shows leptomeningeal and irregular peripheral enhancement, suggestive of meningitis. Diffusion restriction DWI (*B*) and ADC (*C*) maps indicate multiple abscesses. Time-of-flight venogram MIP images (*D, E*) demonstrate loss of flow-related enhancement of the anterior superior sagittal sinus, consistent with venous sinus thrombosis (*arrowheads, D, E*). Notice extensive preseptal and postseptal inflammation in the left orbit (*arrowhead, F*) and opacified ethmoid air cells (*F*). MIP, maximum intensity projection.

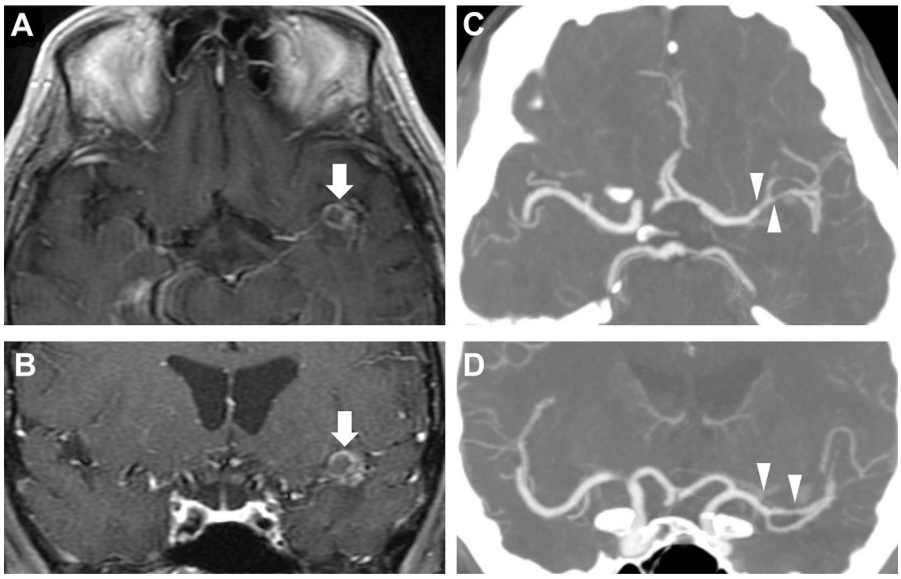

Fig. 26.

Vasculitis in tuberculous meningitis. In a patient with HIV and left-sided retroorbital headaches, T1 postcontrast axial (*A*) and coronal MR images (*B*) reveal a peripherally enhancing lesion in the left perisylvian region (arrows, *A, B*) and faint basilar enhancement, consistent with tuberculous meningitis with tuberculoma. CT angiography (CTA) via axial (*C*) and coronal thin MIP images (*D*) show focal narrowing and irregularity of the distal M1, M2, and proximal M3 segments of the left middle cerebral artery (arrowheads, *C, D*), suggestive of vasculitis secondary to tuberculous meningitis.

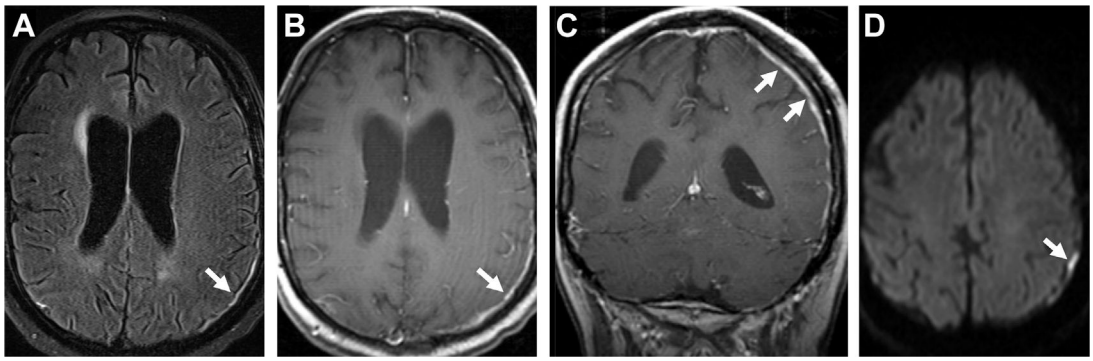

Fig. 27.

Carcinomatous meningitis with dural enhancement in a patient with acute myeloid leukemia. Notice FLAIR hyperintensity (*arrow, A*), and thick dural-based enhancement on T1 postcontrast (*arrows, B, C*) with restricted diffusion (*arrow, D*).

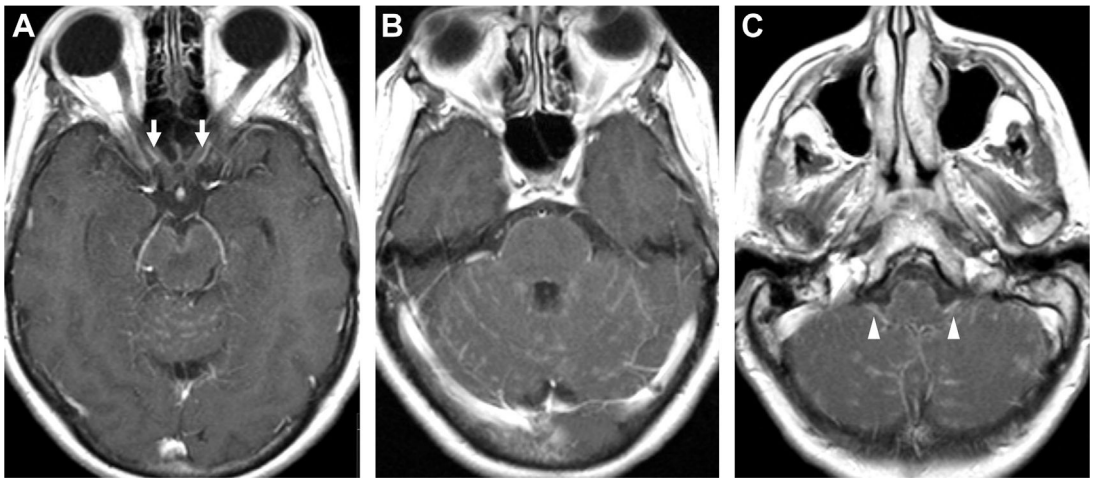

Fig. 28.

Neurosarcoidosis. T1 postcontrast MR imaging demonstrates enhancement of both prechiasmatic optic nerves (*arrows, A*) with patchy linear and nodular enhancement around the brainstem and cerebellum (*B*) and bilateral enhancement of the glossopharyngeal/vagus nerves (*arrowheads, C*).

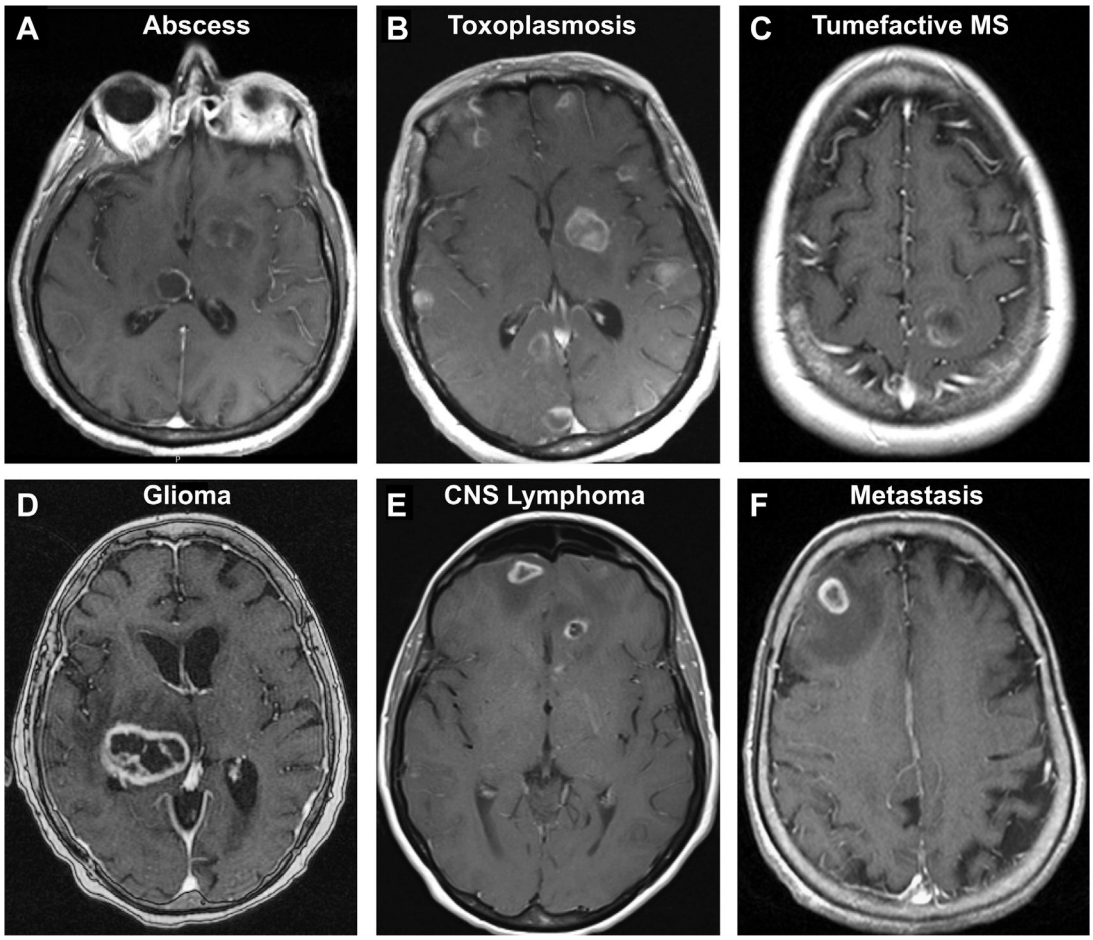

Fig. 29.

Assortment of ring/peripherally enhancing lesions on T1 postcontrast MR imaging. Abscess in an immunocompromised patient (*A*). Multicentric toxoplasmosis (*B*). New demyelinating lesion in tumefactive multiple sclerosis (*C*). Necrotic high-grade glioma (*D*). Multifocal primary CNS lymphoma in an immunocompromised patient with congenital lymphangiectasia (*E*). Junctional metastasis with surrounding edema (*F*).